

# Planarian PTEN homologs regulate stem cells and regeneration through TOR signaling

Néstor J. Oviedo<sup>1,\*</sup>, Bret J. Pearson<sup>2</sup>, Michael Levin<sup>1</sup> and Alejandro Sánchez Alvarado<sup>2,\*</sup>

## SUMMARY

We have identified two genes, *Smed-PTEN-1* and *Smed-PTEN-2*, capable of regulating stem cell function in the planarian *Schmidtea mediterranea*. Both genes encode proteins homologous to the mammalian tumor suppressor, phosphatase and tensin homolog deleted on chromosome 10 (PTEN). Inactivation of *Smed-PTEN-1* and -2 by RNA interference (RNAi) in planarians disrupts regeneration, and leads to abnormal outgrowths in both cut and uncut animals followed soon after by death (lysis). The resulting phenotype is characterized by hyperproliferation of neoblasts (planarian stem cells), tissue disorganization and a significant accumulation of postmitotic cells with impaired differentiation capacity. Further analyses revealed that rapamycin selectively prevented such accumulation without affecting the normal neoblast proliferation associated with physiological turnover and regeneration. In animals in which PTEN function is abrogated, we also detected a significant increase in the number of cells expressing the planarian *Akt* gene homolog (*Smed-Akt*). However, functional abrogation of *Smed-Akt* in *Smed-PTEN* RNAi-treated animals does not prevent cell overproliferation and lethality, indicating that functional abrogation of *Smed-PTEN* is sufficient to induce abnormal outgrowths. Altogether, our data reveal roles for PTEN in the regulation of planarian stem cells that are strikingly conserved to mammalian models. In addition, our results implicate this protein in the control of stem cell maintenance during the regeneration of complex structures in planarians.

## INTRODUCTION

The replacement of cells that are lost to normal physiological turnover relies, in part, on mechanisms that control stem cell number and the efficient, functional integration of their progeny into differentiated tissues. Examples of such tissue homeostasis are provided by the mammalian hematopoietic and digestive systems, in which millions of differentiated blood and epithelial cells expire daily, only to be replaced by the fresh division progeny of resident stem cells (Clarke and Fuller, 2006; Reya and Clevers, 2005). Failure in these processes can lead to a range of dysfunctions, including malignant transformation.

One of the most frequently mutated genes in human cancers is the gene encoding the phosphatase and tensin homolog deleted on chromosome 10 (PTEN) protein (Sansal and Sellers, 2004; Stiles et al., 2004; Sulis and Parsons, 2003). PTEN negatively regulates the phosphatidylinositol-3 kinase (PI3K)-AKT signaling, known to play crucial roles in cellular proliferation, differentiation and migration in both vertebrates and invertebrates (Sulis and Parsons, 2003). In mammals, when PTEN activity is lost in organs displaying high rates of cell turnover, primary and metastatic cancers are detected. Germline mutations of PTEN are found in both Cowden and Bannayan-Riley-Ruvalcaba syndromes (Liaw et al., 1997; Marsh et al., 1997; Marsh et al., 1999; Nelen et al., 1997), and somatic mutations have been associated with Non-Hodgkin's lymphoma (Nakahara et al., 1998), breast, and prostate cancers (Li et al., 1997).

More recently, activation of PI3K and AKT owing to PTEN loss of function has been reported to occur not only in breast, but also in some types of pancreatic, cancers (Asano et al., 2004; Kirkegaard et al., 2005). Thus, a rapidly growing body of evidence suggests a central role for PTEN in the regulation and misregulation of tissue homeostasis in mammals (Marx, 2007).

In invertebrates such as *Drosophila melanogaster* and *Caenorhabditis elegans*, PTEN appears to mainly control cell size and cell cycle during development (Hafen, 2004; Stiles et al., 2004). In *C. elegans*, PTEN (*daf-18*) has been associated with regulation of metabolic rates, longevity and dauer formation (Gil et al., 1999; Mihaylova et al., 1999; Ogg and Ruvkun, 1998). In *Drosophila*, PTEN plays critical roles during development, affecting cell proliferation, and cell and organ size (Gao et al., 2000; Goberdhan et al., 1999; Huang et al., 1999; Oldham et al., 2002). Although studies of PTEN in invertebrates have been highly informative, the study of PTEN in adult tissue homeostasis remains unexplored. As such, models are not yet available to dissect the mechanisms by which human diseases involving PTEN mutations are manifested.

In contrast to flies and nematodes, the adult freshwater planarian *Schmidtea mediterranea* possesses an abundant population of undifferentiated cells, many of which are continuously undergoing cell division. The dividing, undifferentiated cells are known as neoblasts, and the animal derives its robust tissue homeostasis and regenerative properties from both regulating the proliferation of these cells and by determining their division progeny (Newmark and Sánchez Alvarado, 2000). Neoblasts are considered the adult stem cells in planarians because they constantly self-renew and produce daughter cells that will go on to differentiate into all known cell types found in the animal, including the germline (Newmark and Sánchez Alvarado, 2002). In fact, neoblasts are the only known proliferative cell in the flatworm, and their division progeny is instrumental in supporting, and maintaining, differentiated tissues

<sup>1</sup>Center for Regenerative and Developmental Biology, Forsyth Institute, and Developmental Biology Department, Harvard School of Dental Medicine, Boston, MA 02115, USA

<sup>2</sup>Department of Neurobiology and Anatomy, Howard Hughes Medical Institute, School of Medicine, University of Utah, Salt Lake City, UT 84132, USA

\*Authors for correspondence (e-mail: noviedo@drmichaellevin.org; sanchez@neuro.utah.edu)

during physiological cell turnover (Reddien and Sánchez Alvarado, 2004; Sánchez Alvarado, 2006). After amputation, planarians develop a specialized structure at the cut surface, known as a regeneration blastema, which is the result of extensive proliferation by neoblasts.

Here, we report the identification of two *PTEN* orthologs in planarians (*Smed-PTEN-1* and *Smed-PTEN-2*). RNA interference (RNAi) of these genes is lethal; the phenotype is characterized by an inhibition of tissue regeneration, abnormal outgrowths associated with a neoblast-hyperproliferative response, and a lack of cell differentiation and tissue maintenance. Strikingly, we also observed that the abnormalities and lethality detected in worms with RNAi of both *Smed-PTEN* genes [*Smed-PTEN-1*, -2(RNAi) worms] could be prevented by pharmacological treatment with rapamycin (an inhibitor of the protein kinase, target of rapamycin [TOR]), without affecting physiological neoblast proliferation. Because specific upregulation of the planarian *Akt-like* gene (*Smed-Akt*) is detected in RNAi-treated animals and prevented by rapamycin treatment, it is likely that an involvement of the AKT pathway is necessary for the *Smed-PTEN* genes to exert their function. Together, these observations support recent evidence demonstrating that *PTEN* activity can help distinguish differences between normal and abnormal self-renewing mechanisms in stem cells during malignant transformation in mammals (Yilmaz et al., 2006; Zhang et al., 2006). We propose that, in planarians, *PTEN* modulates AKT function and that the abnormalities observed in the *Smed-PTEN* phenotype are due

to both autonomous and non-autonomous stem cell roles of *PTEN*. Additionally, our data revealed that AKT is required for rapamycin to compensate for *PTEN* loss of function. Thus, we propose that planarians may serve as a powerful model system in which to dissect the roles of tumor suppressor activities in regulating stem cell functions.

## RESULTS

### Three *PTEN* homologs exist in *S. mediterranea*

All known *PTEN* homologs share conserved phosphatase and tensin domains (Lee et al., 1999). Initially, we identified potential homologs by performing BLAST searches against the planarian genome with both the fly and human *PTEN* genes. We then took the predicted planarian sequences, which contained both of the conserved domains, and carried out reciprocal BLAST searches against the human and fly genomes. This returned a list of three potential orthologs of *PTEN*.

In addition to *PTEN*, humans possess two other *PTEN*-like genes that contain phosphatase and tensin domains, *TPIP* and *TPTE* (Sulis and Parsons, 2003). To clearly define the orthology between planarian *PTEN*-like genes and the other human homologs, phylogenetic analyses were carried out (see Methods). The results indicate that planaria have two paralogous bona fide *PTEN* orthologs and a gene orthologous to the human *TPTE* and *TPIP* genes (Fig. 1A). cDNAs for both *PTEN* genes had been previously cloned as part of a cDNA sequencing project (Sánchez Alvarado et al., 2002). We will refer to these genes as *Smed-PTEN-1* and *Smed-PTEN-2*.

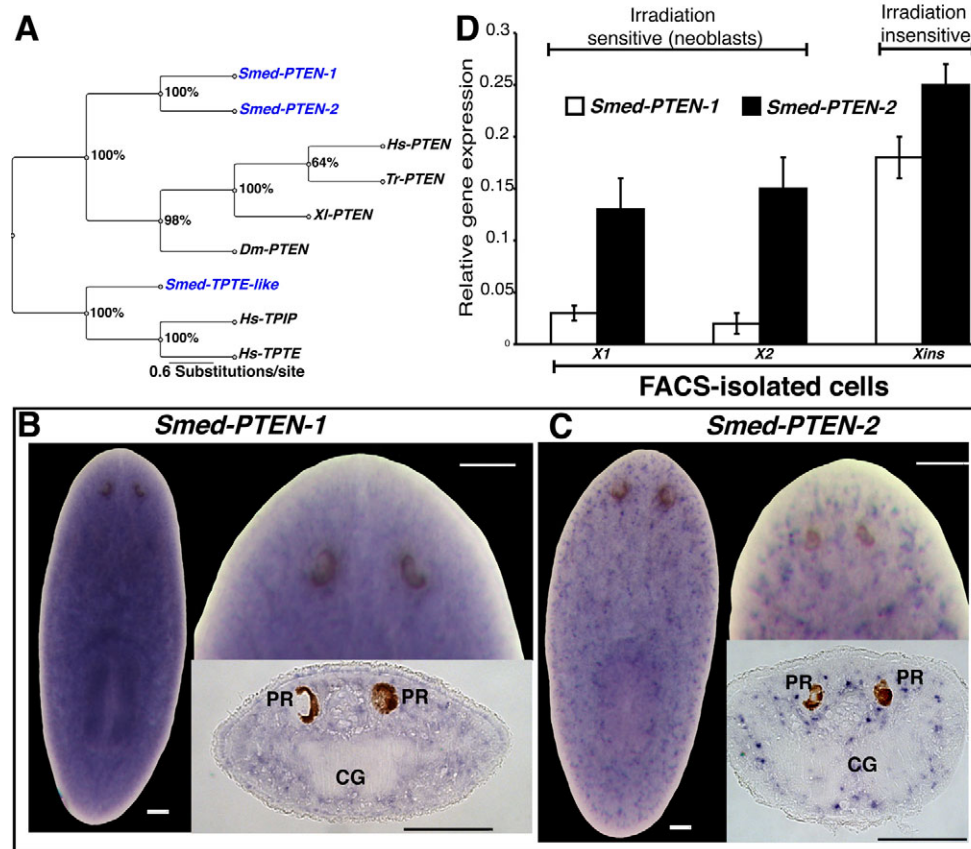


**Fig. 1. *Smed-PTEN* phylogenetics and expression studies.** (A) Bayesian analysis of *PTEN* family members shown as an unrooted tree with relative branch lengths. Bootstrap support is shown for each node. Species used: *Smed* (*Schmidtea mediterranea*), *Hs* (*Homo sapiens*), *Tr* (*Takifugu rubripes*), *Xl* (*Xenopus laevis*), *Dm* (*Drosophila melanogaster*). (B, C) Representative whole-mount ISH in intact worms showing the widely distributed expression patterns (purple precipitation) for both *Smed-PTEN-1* and *Smed-PTEN-2*, respectively. In both cases anterior is at the top; bars, 100 µm. A more detailed view of the expression patterns, including area in front of the photoreceptors, can be visualized at higher magnifications for both genes, as well as from tissue sections. PR: photoreceptors; CG: cephalic ganglia. (D) *Smed-PTEN-1* and *Smed-PTEN-2* qRT-PCR from different cell populations isolated by flow cytometry. Note that both genes are expressed in irradiation sensitive (X1 and X2) and insensitive (Xins) cells, consistent with the wide distribution observed in whole-mount ISH results. Expression levels are relative to the standard internal control clone (*H.55.12e*). Numbers are expressed as the average of triplicate experiments (± s.d.) from two different preparations.

### Smed-PTEN genes are expressed in neoblasts and differentiated cells

The general expression patterns of *Smed-PTEN-1* and *Smed-PTEN-2* were defined using whole-mount *in situ* hybridizations (ISH). Expression for both genes (Fig. 1B,C) is detected throughout mesenchymal tissues (dorsal/ventral and anterior/posterior), including postmitotic areas (i.e. the area in front of the photoreceptors and the pharynx). No obvious restriction to a particular organ system was observed; however, spatial expression patterns differ in that the *Smed-PTEN-1* signal is dispersed, whereas *Smed-PTEN-2* expression is detected in defined clusters throughout the mesenchyme (Fig. 1B,C). Expression patterns were confirmed as specific by performing several optimization rounds of the ISH protocol and standardizing the results with control probes of known expression patterns. Additionally, ISH with sense probes in wild-type worms and antisense probes in RNAi worms, for each *Smed-PTEN* gene confirmed the detected expression patterns (supplementary material Fig. S1 and data not shown).

Because the spatial signal distribution precluded us from defining the cell types expressing *Smed-PTEN-1* and *Smed-PTEN-2*, we performed quantitative real-time PCR (qRT-PCR) analyses on diverse cell populations isolated by fluorescence activated cell sorting (FACS) (Fig. 1D). We tested the irradiation-sensitive cells comprised by the X1 and X2 populations, and the irradiation-insensitive cell types represented by the Xins area of the FACS profile (Hayashi et al., 2006; Reddien et al., 2005b). These experiments revealed that expression of both *Smed-PTEN* genes is detectable in all three cell subpopulations (Fig. 1D). These data suggest that the expression of *Smed-PTEN-1* and *Smed-PTEN-2* is widespread and includes neoblasts.

### Silencing of *Smed-PTEN-1* and *Smed-PTEN-2* results in abnormal tissue growth and lethality

RNAi experiments were performed to abolish the expression of each *Smed-PTEN* gene individually or simultaneously. We designed and optimized a double-stranded RNA (dsRNA) microinjection schedule that consistently reproduces a particular phenotype (see below). This procedure requires a total of five microinjections distributed through 11 days (Fig. 2A). The dsRNA was synthesized in vitro according to standard protocols (Sánchez Alvarado and Newmark, 1999) and injected at different intervals during the schedule (Fig. 2A). Throughout the experiment, all groups were extensively evaluated under the microscope and scored for anatomical and/or behavioral changes (Reddien et al., 2005a). Additionally, abrogation of gene expression was confirmed by RT-PCR and whole-mount ISH (supplementary material Fig. S1 and data not shown).

Representative results from different groups of animals, 12 days after the first microinjection, are shown in Fig. 2B. Planarians injected with water (control), dsRNA-*Smed-PTEN-1* or dsRNA-*Smed-PTEN-2* were indistinguishable from each other (Fig. 2B left panels). In contrast, all *Smed-PTEN-1, -2(RNAi)* worms ( $n > 100$ ) displayed behavioral and anatomical changes followed by death (100% penetrance). Signs of the phenotype began with a slowing of movements and a lack of normal photophobic response, followed by reabsorption of the most anterior area in front of the photoreceptors (head regression). Head regression in planarians is associated with impaired neoblast function (Guo et al., 2006;

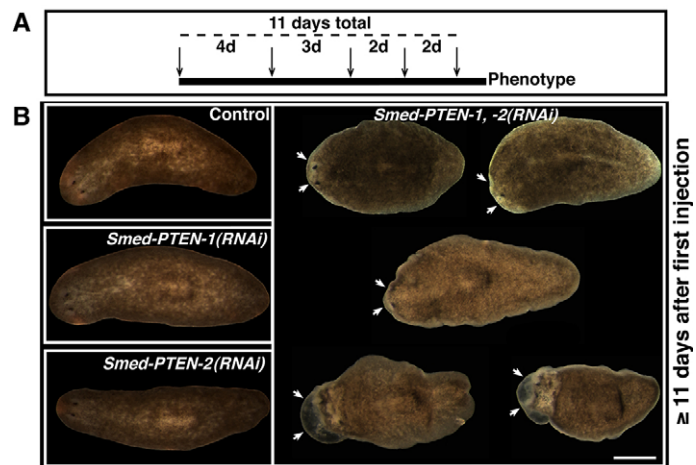


**Fig. 2. Microinjection schedule and its effect in intact planarians.** (A) Microinjection schedule in intact planarians. A total of five injections (arrows) were performed during 11 days (dashed line). Injections were administered at different intervals (days), illustrated by numbers between arrows. (B) Representative images from experimental groups following 11 or more days after the first injection. Conditions shown: control (water-injected), *Smed-PTEN-1(RNAi)*, *Smed-PTEN-2(RNAi)* and simultaneous *Smed-PTEN-1, -2(RNAi)*. We did not observe any external differences between the first three conditions (left column), while in simultaneous RNAi animals important behavioral and macroscopic abnormalities were noted. Initial signs of the phenotypes (illustrated from top left to bottom, white arrows) began with lethargic movements and tissue regression in front of the photoreceptors, followed by development of external outgrowths and lysis. In all cases anterior end is to the left. Bar, 500  $\mu$ m.

Reddien et al., 2005a; Reddien et al., 2005b); however, this phenotype is normally accompanied by a characteristic ventral curling, which did not occur at any time in *Smed-PTEN-1, -2(RNAi)* worms. Instead, as the phenotype progressed, abnormal growths became evident in different body parts, but tended to be more severe at anterior ends (Fig. 2B, arrows). These abnormal growths increased rapidly in size and number, and worms eventually began to lyse and die three to four days after the first obvious signs of the phenotype (supplementary material Table S1). In the majority of cases, these changes were most evident after the final injection ( $11 \pm 2.2$  days after the first injection, average  $\pm$  standard deviation [s.d.]); representative images of the phenotype (12 days after first injection) with different degrees of severity are shown in Fig. 2B (right panel). These data indicate that *Smed-PTEN-1* and *Smed-PTEN-2* functionally compensate each other, and that these genes play a role in regulating proper neoblast functions that may differ from those observed following either irradiation or silencing of *smedwi-2* (a gene involved in the regulation of planarian stem cells) (Reddien et al., 2005b).

### *Smed-PTEN-1* and *Smed-PTEN-2* are required for regeneration

To determine whether *Smed-PTEN* genes play a role during regeneration, we performed an RNAi time-course strategy similar to that carried out in intact worms, except that animals were amputated at pre/postpharyngeal levels one day after the third injection (Fig. 3A). Trunk fragments resulting from these amputations received two additional injections (days 1 and 3 post-amputation);

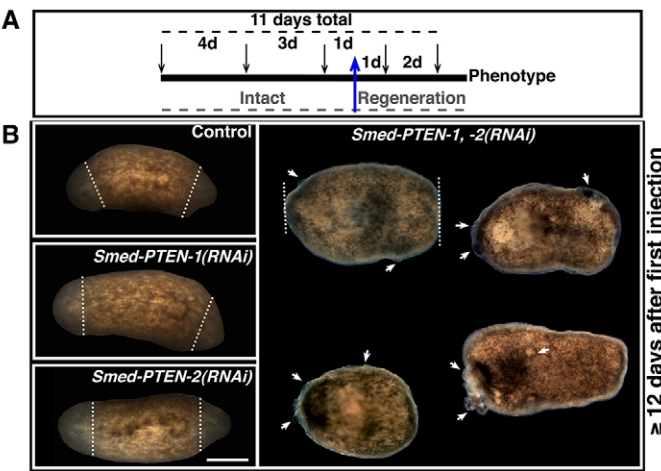


**Fig. 3. Microinjection schedule and its effects during tissue regeneration.** (A) Microinjection schedule. A total of five injections (arrows) were performed during 11 days (top dashed line). Injections were administered at different intervals (numbers between arrows). The blue arrow depicts the stage at which bipolar amputation was performed and the dashed line (gray) at the bottom highlights the experimentation period during which animals were either intact or under regeneration. (B) Representative images of experimental groups between three and eight days post-amputation (the amputation level is represented by the white dashed line). Conditions shown: control (water-injected), *Smed-PTEN-1(RNAi)*, *Smed-PTEN-2(RNAi)*, and simultaneous *Smed-PTEN-1, -2(RNAi)*. No external differences were observed during anterior or posterior blastema formation (unpigmented tissue formed after amputation) between the first three conditions (left column), whereas in simultaneous RNAi fragments, important behavioral and macroscopic abnormalities were noted ( $n=47/47$  worms, similar numbers for each group were run in parallel). Abnormal outgrowths (white arrows) were evidenced in different parts of the animal (including the tissue surrounding the amputation area) followed by lysis shortly after visualization of the first sign of the phenotype. In all cases anterior is to the left. Bar, 500  $\mu$ m.

subsequent behavioral and anatomical changes were evaluated (Reddien et al., 2005a). Animals subjected to either *Smed-PTEN-1(RNAi)* or *Smed-PTEN-2(RNAi)* developed anterior and posterior regeneration blastemas, with macroscopic regenerative dynamics that were indistinguishable from those observed in control animals (i.e. normal wound healing, blastema formation, photoreceptor pigmentation, photophobic response, etc.; Fig. 3B, left panels). In contrast, the *Smed-PTEN-1, -2(RNAi)* worms showed normal wound healing, but failed to form blastemas and by approximately the second day post-amputation ( $10\pm0.8$  days after the first injection) signs of the phenotype (no blastema formation, scattered outgrowths) were evident in all animals ( $n=47/47$ ). These abnormal growths multiplied and within one week after amputation ( $6.25\pm3.3$  days) all animals were dead (Fig. 3B, right panel). These results are consistent with the effect observed for *Smed-PTEN-1, -2(RNAi)* in intact worms (supplementary material Table S1). Furthermore, in both uncut and regenerating animals, overt signs of the phenotype were noted at similar times after the first injection (~11 days; Student's *t*-test,  $P=0.25$ ), suggesting that under these conditions amputation does not influence phenotype dynamics. These results support our previous conclusion that *Smed-PTEN-1* and *Smed-PTEN-2* are required for proper neoblast function and indicate that the planarian PTEN orthologs are necessary for blastema formation.

### Disorganization of differentiated tissues and cellular infiltration occur in the absence of PTEN function

We sought to better understand the cellular basis for the observed phenotype in *Smed-PTEN-1, -2(RNAi)* animals. We first performed fluorescent immunohistochemistry with antibodies specific to differentiated tissues, specifically neurons, muscle and cilia (Cebrià et al., 1996; Robb and Sánchez Alvarado, 2002; Sakai et al., 2000). Results from these experiments revealed unexpected and severe disruptions to the anatomical and functional integrity of these tissues (Fig. 4). Photoreceptor neurons were found in disarray, and were often dispersed and lacking optic chiasmata (Fig. 4A); body wall musculature displayed areas devoid of myosin positive cells (Fig. 4B); and the surface area of dorsal cilia fields was reduced (Fig. 4C). Such defects are consistent with the idea that tissue maintenance by neoblasts and their progeny are compromised after silencing of *Smed-PTEN-1* and *Smed-PTEN-2*.

Histological analyses of RNAi-treated animals not only confirmed the tissue disorganization detected by immunohistology, but also uncovered discontinuities in the basement membrane (BM) and the presence of abnormal invasive cells (Fig. 4D,E). The BM (extracellular matrix underneath the epithelial cells; Fig. 4D, lower arrows) separates the epithelium from the underlying mesenchyme (Nelson and Bissell, 2006). In the *Smed-PTEN-1, -2(RNAi)* animals, the integrity of the BM is markedly disrupted, and in some areas a physical barrier separating epithelial cells and mesenchymal tissues cannot be detected (Fig. 4E, top right). Such direct contact between epithelium and mesenchyme is also observed in planarians during normal wound healing after amputation and is known to be involved in the proliferation of nearby neoblasts (Hori, 1979a; Hori, 1979b; Hori, 1980). This may explain, in part, the overproliferation of cells detected in *Smed-PTEN-1, -2(RNAi)* animals.

The abnormal invasiveness of some cells in *Smed-PTEN-1, -2(RNAi)* animals was readily apparent in the pharynx (Fig. 4E, bottom right). Normally, postmitotic progeny of neoblasts migrate to the epithelium and pharynx to replace cells lost during cellular turnover and tissue regeneration (Newmark and Sánchez Alvarado, 2000). Although, in the *Smed-PTEN* phenotype no ectopic mitotic activity was noted (i.e. no mitotic figures were detected in front of the photoreceptors or pharynx; see Fig. 4G), the cellular infiltration (i.e. increase in cellularity in different organs) observed in the epithelium and pharynx (Fig. 4E) may be due to the migration of neoblast progeny. Bromodeoxyuridine (BrdU) experiments confirmed that the migratory ability of the neoblast progeny was not lost after abrogation of *Smed-PTEN* genes (data not shown). Additionally, these cellular infiltrations were characterized by the presence of basophilic cells (Fig. 4E).

### *Smed-PTEN-1* and *Smed-PTEN-2* affect neoblast proliferation and cell number

To further characterize the *Smed-PTEN-1, -2(RNAi)* phenotype, we examined whether cell number and the anatomical composition of different tissue types were affected. First, we dissociated control and *Smed-PTEN-1, -2(RNAi)* planarians ( $n=10$  for each group) into cell suspensions of equal volume. The cells were spotted onto slides and the nuclei counterstained with propidium iodide (PI) (see experimental procedures for details). PI signal quantification revealed an increase of ~20% in cell number in *Smed-PTEN-1,*

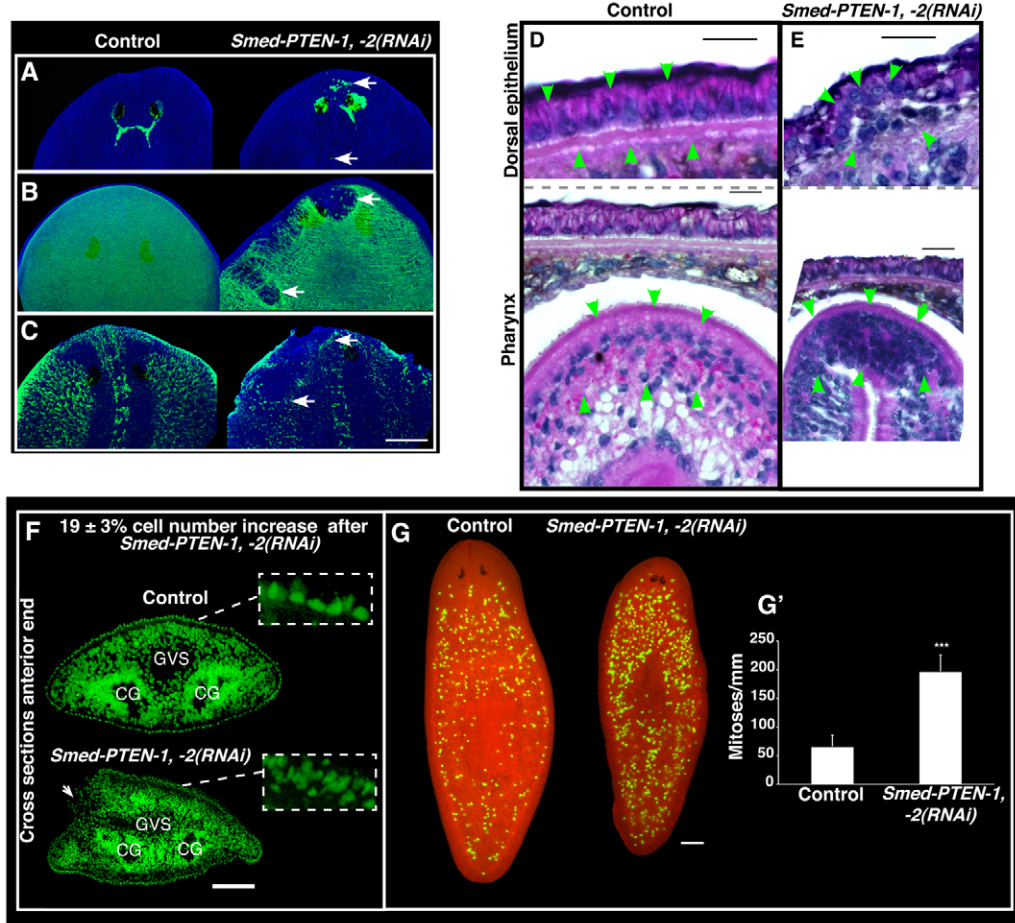


**Fig. 4. The *Smed-PTEN* phenotype is characterized by a lack of tissue maintenance, tissue architecture disorganization and neoblast hyperproliferation.** (A-C) Representative confocal images (anterior, dorsal views) from control (water-injected) worms (left column in A-C) and *Smed-PTEN-1, -2(RNAi)* worms (right column), respectively. Immunostaining was performed by using different tissue markers: neuronal marker (anti-arrestin, VC-1) (A); muscle (anti-myosin heavy chain, TMUS-13) (B); and epithelium (anti- $\alpha$ -acetylated tubulin) (C) antibodies, respectively. White arrows are used to indicate morphological disruptions. Bar, 100  $\mu$ m. (D, E) Tissue disorganization and cellular infiltration in the *Smed-PTEN* phenotype. Representative images of paraffin-tissue sections stained with hematoxylin and eosin from control (D) and *Smed-PTEN-1, -2(RNAi)* (E) worms showing similar anatomical areas, illustrating dorsal epithelium (prepharyngeal area) and pharynx. Green arrowheads in the top panel of (D) indicate the columnar epithelium and basement membrane of control animals. The green arrowheads in the top panel of (E) denote the multiple cell layers in the epithelium and the disruption of basement membrane in *Smed-PTEN-1, -2(RNAi)* animals. The bottom panels illustrate cross-sections of the dorsal epithelium of the pharyngeal area, along with part of the pharynx (the large ovoid-shaped structure). Note the cellular infiltration in the pharynx of *Smed-PTEN-1, -2(RNAi)* worms, with cells possessing morphology similar to that described for neoblasts (i.e. rounded cells with large nuclei and scant cytoplasm), consistent with a neoblastoma (Best and Morita, 1982). Bars, 20  $\mu$ m. (F) Cross sections (10  $\mu$ m thickness) of the anterior end, with nuclei counterstaining (Sytex green) in both control worms (top) and *Smed-PTEN-1, -2(RNAi)* worms (>12 days after the first dsRNA injection (bottom)). Notice the anatomical disruption (white arrow) and the multiple cell layers of the epithelium (insets). Numbers represent the total count from nuclei counterstaining in control ( $n=730$ ) and *Smed-PTEN-1, -2(RNAi)* worms ( $n=902$ ), after a pool of worms ( $n=10$ ) were dissociated (average of cells from three experiments  $\pm$  s.d.). Dorsal side is to the top. CG: cephalic ganglia; GVS: gastrovascular system. Bar, 0.2 mm. (G) Representative images of whole-mount immunostaining using  $\alpha$ -phosphorylated histone H3 (H3P) antibody in intact worms (12 days after first injection). Control (water-injected) and *Smed-PTEN-1, -2(RNAi)* worms are shown. (G') H3P-signal quantification from both control and simultaneous *Smed-PTEN-1, -2(RNAi)* worms. A significant increase ( $P<0.0001$ ) in mitotic activity was observed in RNAi treated animals. Mitotic activity in control worms and following individual *Smed-PTEN* RNAi treatments was qualitatively and quantitatively indistinguishable between the groups (data not shown). Results represent average  $\pm$  s.d. from  $n\geq 10$  worms in each condition.

*-2(RNAi)* worms; however, this increase in cell number was not associated with increases in animal length or cell size (Fig. 4F and data not shown). Qualitative anatomical analyses (visual inspection of nuclei counterstaining using Sytex green, Molecular Probes) were also performed in cross-sections of different areas (anterior, posterior) and revealed that the increase in cell number/density in the *Smed-PTEN-1, -2(RNAi)* phenotype was scattered rather than restricted to a specific tissue or organ (data not shown). However,

in animals with a severe phenotype ( $n=5$ ), we observed evidence for the occurrence of hyperplasia, in which the normally monolayered epidermis became multilayered in *Smed-PTEN-1, -2(RNAi)* animals (Fig. 4F). This finding is consistent with previous chemically-induced epithelial hyperplasia observed in planarian neoplasms (Foster, 1963).

Because neoblasts are the only known proliferative cell type in asexual planarians, we sought to evaluate whether cell proliferation

was involved in the increase in cell number observed in *Smed-PTEN-1, -2(RNAi)* animals. We assayed whole animals with an anti-phosphorylated histone-3 (H3P) antibody that specifically labels mitotic neoblasts (Newmark and Sánchez Alvarado, 2000). When signs of the *Smed-PTEN* phenotype became visible (12 days after the first injection, as described above), mitotic activity was quantified (Reddien et al., 2005a; Reddien et al., 2005b) in four different groups: 1) control; 2) *Smed-PTEN-1(RNAi)*; 3) *Smed-PTEN-2(RNAi)* and 4) *Smed-PTEN-1, -2(RNAi)*. We found no differences in mitotic activity between control animals and animals in which the *Smed-PTEN* genes were individually silenced (data not shown). However, a significant increase in mitotic cells (Student's *t*-test,  $P<0.001$ ) was observed in *Smed-PTEN-1, -2(RNAi)*

animals (Fig. 4G). These data suggest that loss of PTEN activity in planarians leads to hyperproliferation and may be responsible for the observed hyperplasia (Fig. 4F).

#### *Smed-PTEN-1 and Smed-PTEN-2 regulate neoblast differentiation*

To better understand the nature of the effects exerted by PTEN on neoblasts, we tested several markers associated with neoblast function. First, we carried out a quantitative analysis based on ISH, performed in dissociated control and *Smed-PTEN-1, -2(RNAi)* animals, which revealed that there was an important increase in cells expressing neoblast markers after abrogation of both *Smed-PTEN* genes (supplementary material Fig. S2). This suggests that, in addition to an increase in mitotic activity, the

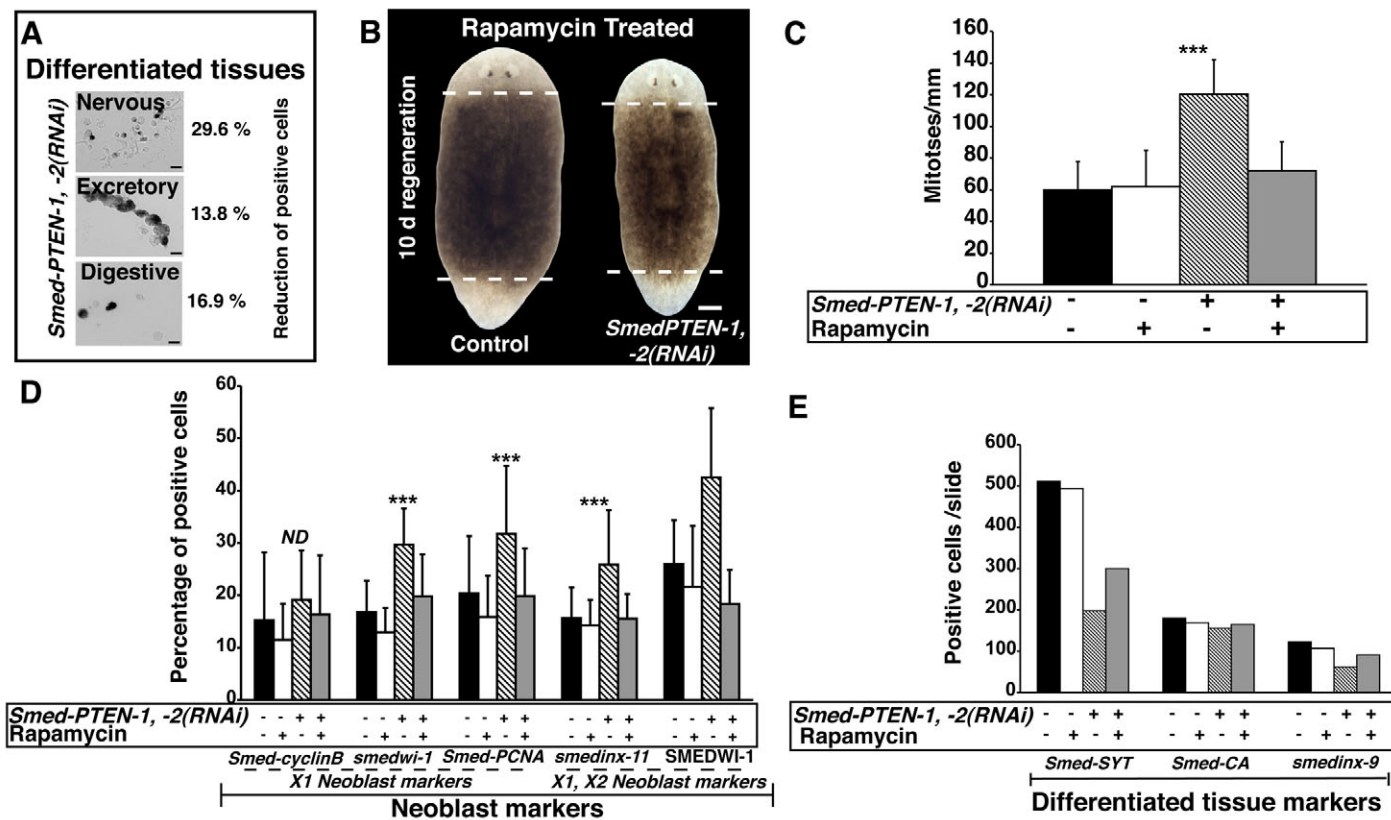
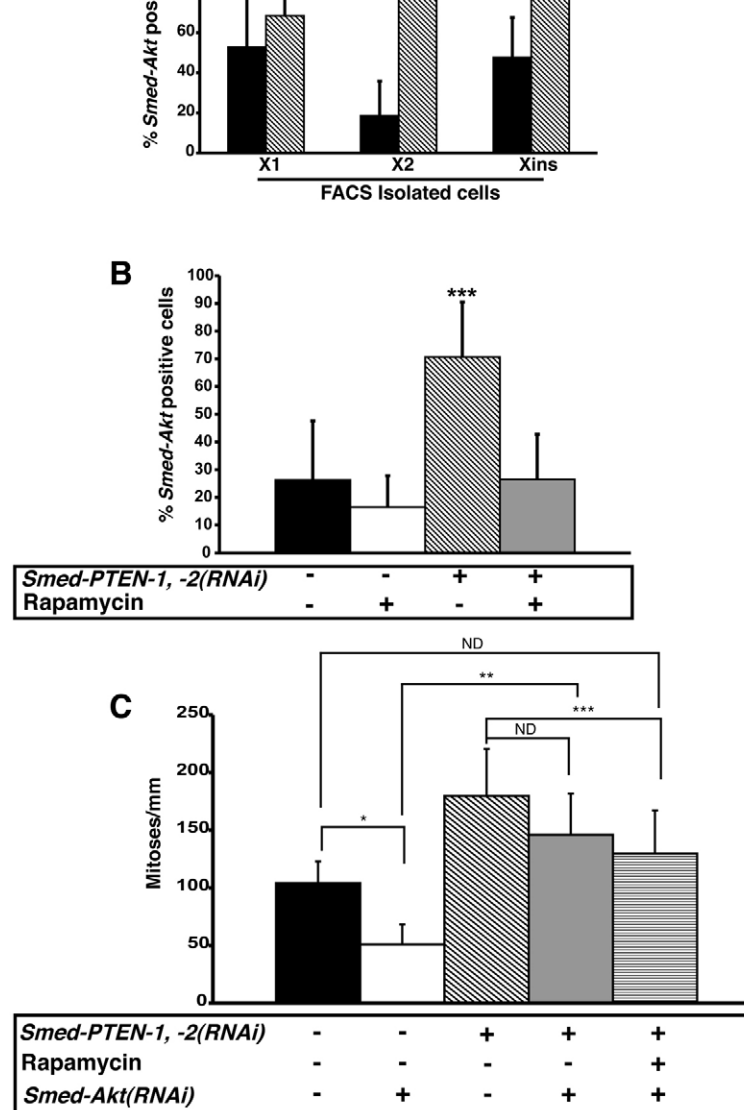


**Fig. 5. PTEN-RNAi disrupts tissue maintenance and rapamycin treatment compensates for *Smed-PTEN* loss.** (A) Quantification of cells expressing markers of differentiated tissues. From a pool of dissociated animals, ISH was performed using probes specific to the nervous (synaptotagmin, *Smed-Syt*), excretory (carbonic anhydrase, *Smed-CA*) and digestive (*smedinx-9*) systems. Representative pictures of cells expressing each marker are shown (black precipitation). Cells expressing each marker were counted and the average of two independent experiments was recorded as the total number of positive cells per slide: *Smed-Syt*,  $n=608$  and  $n=428$ ; *Smed-CA*,  $n=109$  and  $n=94$ ; *smedinx-9*,  $n=142$  and  $n=118$  for control and *Smed-PTEN-1, -2(RNAi)* worms, respectively. Respective percentage reductions in the number of expressing cells after RNAi are shown. (B) Rapamycin treatment prevents abnormal outgrowths, lethality and rescues regenerative events in RNAi-treated animals. Worms subjected to *Smed-PTEN-1, -2(RNAi)* were unable to regenerate, external outgrowths were evident, and the worms failed to survive longer than 7 days post-amputation ( $n=27/27$ ), whereas rapamycin-treated *Smed-PTEN-1, -2(RNAi)* or control worms developed anterior and posterior blastemas, and survived for more than one month after the first dsRNA injection ( $n=29/29$ ). Representative images of rapamycin-treated control and *Smed-PTEN-1, -2(RNAi)* worms are shown. (C) Quantification of mitotic activity. Note that control and rapamycin-treated worms show similar levels of mitotic activity and that in *Smed-PTEN-1, -2(RNAi)* worms, proliferation was higher (\*\* $P<0.01$ ). However, simultaneous *Smed-PTEN* RNAi and rapamycin treatment prevent abnormal proliferation while keeping proliferative activity similar to control animals. Displayed values represent average  $\pm$  s.d. of  $n\geq 8$  worms per condition, for at least two independent replications. (D) Expression of neoblast markers in dissociated worms. An increase in the number of cells expressing each neoblast marker was always observed in *Smed-PTEN-1, -2(RNAi)* worms after the RNAi treatment, but was prevented with rapamycin treatment (Student's *t*-test, \*\* $P<0.001$ ). (E) Expression of differentiated tissue markers in dissociated worms. The same pools of animals discussed in Fig. 5D were used to perform ISH with genes expressed in differentiated tissues (*Smed-SYT*, *Smed-CA* and *smedinx-9*). For panels (D) and (E), dissociations were performed from a pool of ten animals per group and cell numbers represent the average  $\pm$  s.d. of 20 different fields per slide with an objective of  $20\times$  magnification. Total numbers of cells expressing each gene per slide are shown. ND: no difference.

number of cells expressing neoblast-specific markers increased in the *Smed-PTEN* phenotype. In contrast, a marked reduction in the expression of markers for differentiated cells such as neuronal (*Smed-SYT*), excretory (*Smed-CA*) and digestive (*smedinx-9*) cells was observed in *Smed-PTEN-1, -2(RNAi)* animals (Fig. 5A). We independently confirmed these results by qRT-PCR (supplementary material Table S2). The measured increment in the numbers of both proliferative neoblasts and their postmitotic progeny is consistent with the increase in cell numbers detected histologically (Fig. 4F and supplementary material Fig. S2) in *Smed-PTEN-1, -2(RNAi)* worms. Taken together, the data indicate that loss of *Smed-PTEN* function is characterized by an increase in neoblast numbers, but also a decrease in differentiated tissues – probably owing to an inability of the neoblast progeny to properly differentiate.



### Rapamycin prevents abnormalities produced by *Smed-PTEN* loss of function

PTEN loss of function is associated with activated PI3K-Akt signalling pathway in many malignancies related to cancer. The macrolide rapamycin operates through the multicomplex protein TOR, and has been shown to be effective in reversing the symptoms observed in PTEN loss of function models (Guertin and Sabatini, 2007; Sabatini, 2006; Yilmaz et al., 2006). We sought to test whether the effects of rapamycin in mammals could be recapitulated in planarians (see experimental procedure for details).

Planarians subjected to RNAi of both *Smed-PTEN* genes and, subsequently, to daily injections of rapamycin, failed to develop any macroscopic signs of the characteristic *Smed-PTEN* phenotype, either in the first two weeks ( $n=50/50$ ), or after one month of treatment ( $n=19/20$ ). However, exposure to rapamycin restored the

**Fig. 6. *Smed-Akt* expression analyses in *Smed-PTEN* phenotype and proliferative activity in triple RNAi worms.** (A) *Smed-Akt* expression in FACS-isolated cells from control and *Smed-PTEN-1, -2(RNAi)* worms at day 12 after the first injection ( $n=10$  per group). ISH was performed in FACS-isolated cells from control and *Smed-PTEN-1, -2(RNAi)* worms; cells expressing *Smed-Akt* were quantified for each fraction (see Methods). In control animals, *Smed-Akt* expression levels are highest in fractions X1 and Xins and comparable to each other (Student's *t*-test, \*\* $P=0.24$ ), whereas *Smed-Akt* expression is lowest in the X2 fraction (Student's *t*-test,  $P<0.0001$ ). In animals treated with dsRNA against both *Smed-PTEN* paralogs, significant increases in *Smed-Akt* expressing cells are observed, relative to control worms, with the greatest increase observed in the X2 fraction (Student's *t*-test, \*\*\* $P<0.0001$ ). (B) *Smed-Akt* expression in dissociated worms. Pools of animals ( $n=10$  each) that had been treated with RNAi, rapamycin, or both, were dissociated and cells expressing *Smed-Akt* were quantified. *Smed-PTEN-1, -2(RNAi)* animals showed the highest number of *Smed-Akt* expressing cells (Student's *t*-test, \*\*\* $P<0.0001$ ). Rapamycin treatment in *Smed-PTEN-1, -2(RNAi)* worms prevented the increase in *Smed-Akt* expressing cells, but maintained a similar number to control animals (Student's *t*-test,  $P=0.5$ ). (C) Mitotic activity in *Smed-Akt(RNAi)* worms, *Smed-PTEN-1, -2(RNAi)* worms or triple RNAi worms, with or without rapamycin treatment. Animals were processed for immunostaining 10 days after the first dsRNA-*PTEN* injection. Mitotic cells were detected in whole animals with H3P antibody and the signal quantified as described in the Methods ( $n>6$  animals/condition). *Smed-Akt(RNAi)* worms showed a reduced number of mitotic cells relative to control worms (Student's *t*-test, \* $P<0.002$ ). Although, the hyperproliferative defects observed in the *Smed-PTEN* phenotype were not prevented in triple RNAi worms (Student's *t*-test, \*\* $P=0.3$ ), mitotic activity was significantly reduced to levels comparable with control animals (control vs. triple RNAi, rapamycin,  $P=0.5$ ; *Smed-PTEN-1, -2(RNAi)* vs. triple RNAi, rapamycin, Student's *t*-test, \*\*\* $P=0.002$ ). ND: no difference.

ability of *Smed-PTEN-1, -2(RNAi)* animals to launch a regenerative response after amputation, i.e. rapamycin treatment restored neoblast proliferation in response to injury. RNAi-treated animals developed anterior and posterior blastemas with the same dynamics as controls ( $n=30/30$ ), and survived for longer than two weeks after the first dsRNA injection (Fig. 5B). After suspending rapamycin treatment, only a fraction of worms developed signs of the *Smed-PTEN* phenotype within one month ( $n=7/19$ ), indicating that the effect of rapamycin treatment perdures for several weeks. Moreover, similar levels of mitotic activity were observed among control worms, worms treated with rapamycin alone, and *Smed-PTEN-1, -2(RNAi)* worms receiving rapamycin, suggesting that rapamycin treatment does not affect basal neoblast proliferation, but specifically prevents abnormal proliferation in the absence of functional *Smed-PTEN* genes (Fig. 5C).

To further evaluate the effects of rapamycin in planarians, gene expression analyses were performed using markers of proliferative and postmitotic progeny of neoblasts (Fig. 5D). The results revealed that the percentage of cells expressing proliferative and postmitotic markers is similar between the control groups and rapamycin-treated *Smed-PTEN-1, -2(RNAi)* worms. However, the expression of differentiated tissue markers was lower in *Smed-PTEN-1, -2(RNAi)* worms treated with rapamycin than in control worms, or in worms receiving rapamycin alone (Fig. 5E), indicating that rapamycin may not fully rescue gene expression in differentiated tissues. Altogether, these results suggest that rapamycin treatment prevents the tissue homeostasis and regeneration defects observed in *Smed-PTEN-1, -2(RNAi)* animals.

#### ***Smed-Akt* expression is upregulated in the *Smed-PTEN* phenotype**

The oncprotein kinase Akt is an important downstream target in the PI3K pathway that has central roles in PTEN loss of function (Guertin and Sabatini, 2007; Sabatini, 2006). Thus, we identified and cloned the planarian *Akt* ortholog (*Smed-Akt*). Unlike PTEN, there is a single *Akt* gene in *S. mediterranea*. *Smed-Akt* expression is widely distributed through the mesenchyme including postmitotic areas and in some cell clusters around the cephalic ganglia (supplementary material Fig. S3).

The wide distribution of the *Smed-Akt* signal was also confirmed by expression analyses of FACS-isolated cells revealing that *Smed-Akt* is expressed in approximately 50% of the cells in both the X1 (proliferating) and Xins (differentiated) fractions, whereas only approximately 20% of the cells in X2 express *Smed-Akt* (Fig. 6A). Strikingly, the distribution of *Smed-Akt* expression was dramatically altered after simultaneous abrogation of both *Smed-PTEN* genes (Fig. 6A), increasing significantly in the X1 and X2 compartments (1.3- and 4.2-fold, respectively), and in differentiated cells (Xins=1.6-fold). In fact, the increase in *Smed-Akt* positive cells was higher than that of any other neoblast marker (Fig. 5D), indicating that *Smed-PTEN-1* and -2 play a role in regulating *Smed-Akt* expression in both neoblasts and cells of differentiated tissues. Furthermore, rapamycin treatment of *Smed-PTEN-1, -2(RNAi)* worms specifically prevents the abnormal increase of *Smed-Akt* signal, while maintaining its basal expression (Fig. 6B and C). Thus, rapamycin is not stochastically downregulating *Smed-Akt* expression, but it is effective in distinguishing between physiological levels of *Smed-Akt* and its abnormal expression after RNAi of *Smed-PTEN-1* and *Smed-PTEN-2*.

#### **RNAi of *Smed-Akt* does not recapitulate the *Smed-PTEN* phenotype**

To evaluate the function of *Akt* in the *Smed-PTEN* phenotype, RNAi experiments involving *Smed-Akt* and *Smed-PTEN* genes were carried out. At the gross morphological level, *Smed-Akt(RNAi)* animals displayed only locomotion defects (~12 days after first injection,  $n=40/40$ ), and did not develop other external abnormalities or head regression even after more than one month (data not shown). *Smed-Akt(RNAi)* animals, however, displayed lower number of proliferative cells when compared with control animals (Student's *t*-test,  $P<0.002$ ), suggesting that *Smed-Akt* is necessary to maintain basal proliferation levels (Fig. 6C). Nevertheless, *Smed-Akt(RNAi)* animals are still capable of forming blastemas after amputation and regenerate with similar dynamics as control animals (data not shown,  $n=30/30$ ). Together, the data indicate that *Smed-Akt* is not sufficient to affect either long-term homeostasis or tissue regeneration.

Worms subjected to triple RNAi [*Smed-Akt(RNAi)*; *Smed-PTEN-1, -2(RNAi)*], with or without rapamycin treatment, failed to display head regression as observed in the *Smed-PTEN* phenotype, yet developed abnormal outgrowths and lethality with full penetrance ( $n=23/23$ , supplementary material Fig. 4). Moreover, the number of proliferating cells in triple RNAi worms and in *Smed-PTEN-1, -2(RNAi)* worms were not statistically different (Student's *t*-test,  $P>0.3$ ). These results suggest that abrogating *Smed-Akt* is not enough to prevent the abnormal hyperproliferation observed in the *Smed-PTEN* phenotype. Surprisingly, after rapamycin treatment, the number of proliferative cells in triple RNAi worms was the same as in the control group (Student's *t*-test,  $P>0.4$ ), although rapamycin treatment failed to prevent abnormal outgrowths ( $n=15/15$ , Fig. 6C and supplementary material Fig. S4). Altogether these data suggest that, irrespective of proliferative levels, functional abrogation of *Smed-PTEN* is sufficient to induce abnormal outgrowths. Additionally, functional disruption of both *Smed-Akt* and *Smed-PTEN* genes reduce the capacity of rapamycin to prevent the abnormalities observed in the *Smed-PTEN* phenotype, suggesting that to be fully effective, rapamycin treatment requires functional *Akt*.

#### **DISCUSSION**

The analyses described here reveal details of the striking evolutionary conservation of PTEN function in stem cell regulation. Our data confirm that *S. mediterranea* offers unique opportunities to dissect, on a molecular basis, conserved, complex signaling pathways affecting adult somatic stem cells during homeostasis, disease, and uniquely, regeneration. Moreover, the *Smed-PTEN* phenotype enables both the identification of factors controlling adult stem cells in tumor generation, and the opportunity to explore and test the mechanisms of action of therapeutic drugs that target elements of the PI3K-AKT-TOR pathway.

#### **Multiple PTEN forms exist in *S. mediterranea***

Phylogenetic analysis of the three PTEN-like genes in planaria has lead to two interesting conclusions. Firstly, the analysis shows that planaria have undergone a paralogous duplication of the ancestral, single PTEN gene. The presence of two PTEN genes has not been described in any other invertebrate. Consistent with a relatively recent duplication, is the fact that both paralogs must be inactivated by RNAi to produce a phenotype. Secondly, expansion of the

vertebrate PTEN family into TPTE and TPIP was thought to be vertebrate-specific, because neither *C. elegans* nor Drosophila have a homolog to either of these genes. Surprisingly, planaria have a homolog that appears to be orthologous to both of these genes. These findings provide further evidence that *S. mediterranea* can be a useful invertebrate organism with which to functionally investigate questions involving genes that are present in vertebrates, but absent in Drosophila or *C. elegans*.

### ***S. mediterranea*: a model to study PTEN regulation of adult stem cells during tissue maintenance and regeneration**

Although PTEN and its substrate are evolutionarily conserved, the phenotypes, and endpoints from experimental assays may differ among biological model systems, owing to the ubiquity, complexity, and multiple effectors of the highly branched PI3K pathway (Stiles et al., 2004). This is particularly illustrated by studies on PTEN modulation of chemotaxis in Dictyostelium, signaling pathways in yeast, regulation of metabolic variables, longevity and dauer formation in *C. elegans*, and growth and size determination at the cellular and organ levels in Drosophila (Hafen, 2004; Stiles et al., 2004; Sulis and Parsons, 2003). Nonetheless, in mammals, recent attention has been drawn to the subtle roles that PTEN signaling plays in abnormal stem cell proliferation and its participation in carcinogenesis (Janzen and Scadden, 2006; Polyak and Hahn, 2006; Rossi and Weissman, 2006; Yilmaz et al., 2006; Zhang et al., 2006).

In *S. mediterranea*, the evolutionary conservation of signaling pathways, the experimentally accessible adult stem cell population, and the robust regenerative capabilities of this organism provide a unique model with which to discover the mechanisms that control stem cells during homeostasis, tumorigenesis, and regeneration. Our data demonstrate that *S. mediterranea* provides a new invertebrate model system, in which the functions of different forms of PTEN can be abrogated in the entire adult animal, allowing for analysis of PTEN dysfunction in multiple organs, simultaneously – an experimental approach that is limited in mammalian models (Stiles et al., 2004; Sulis and Parsons, 2003). In addition, investigation of the possible roles of PTEN in the regeneration of complex structures is uniquely facilitated by the planarian model system. Understanding the *in vivo* function of PTEN in adult stem cell regulation is critical in order to design effective therapeutic strategies targeting components of the PI3K-Akt-TOR pathway.

### **Analysis of the stem cells and their microenvironment during malignant transformation can be performed in the *Smed-PTEN* phenotype**

Unlike other invertebrate models (Gao et al., 2000; Goberdhan et al., 1999; Hafen, 2004; Huang et al., 1999; Mihaylova et al., 1999; Ogg and Ruvkun, 1998), abrogation of PTEN function in adult *S. mediterranea* consistently led to visible outgrowths. A central finding of our work is the overproliferation of neoblasts in animals in which both PTEN paralogs have been functionally abrogated. Because neoblasts are the only known dividing cells in planarians, and expression of both *Smed-PTEN-1* and -2 were detected in these cells, it is reasonable to suggest that the observed hyperproliferation (Fig. 4G; Fig. 5C) may be due to autonomous cellular functions of PTEN in the planarian stem cells. Further, elimination of *Smed-Akt* and addition of rapamycin in *Smed-PTEN-1, -2(RNAi)* animals did not prevent migration of the non-mitotic division progeny of

neoblasts; therefore, it is likely that other PTEN-regulated pathways may play a role in this particular aspect of the phenotype. One likely candidate is the integrin-mediated cell spreading and cell migration pathway, which is independent of mammalian TOR (mTOR) and is inhibited by PTEN (Gu et al., 1998). Hence, elimination of PTEN function in non-dividing planarian cells may enhance their migration and explain both tissue infiltration and the prevention of cephalic resorption in rapamycin-treated *Smed-Akt(RNAi); Smed-PTEN-1, -2(RNAi)* animals. Further molecular analyses should help to formally test this possibility.

We also observed a marked disruption of the basement membrane, separating the epithelium from mesenchymal structures, which is accompanied by cellular infiltration and other morphological abnormalities (Fig. 4A-E). Interestingly, alterations of the epithelial-mesenchymal interactions, loss of tissue architecture, and the ensuing abnormal cell behaviors are considered to be both prerequisite and defining events in the progression of most cancers (Nelson and Bissell, 2006). In fact, anatomical alterations of epithelial-mesenchymal interactions represent a triggering signal in malignant transformation (Nelson and Bissell, 2006), as well as a proliferative response in neoblasts upon amputation (Hori, 1979b; Hori, 1980). Thus, we propose that the hyperproliferative response of neoblasts in the *Smed-PTEN* phenotype may be additionally influenced by the disruption of anatomical barriers, and as such could be considered as a non-autonomous cellular effect of PTEN on neoblasts.

In the past, planarians have been used as *in vivo* models for chemical-induced teratogenesis, and many of these studies led to the proposal that the hyperproliferative response of neoblasts to mutagenic compounds bears some resemblance to teratomas caused by embryonic stem cells, as well as benign and malignant tumors in mammals (Best and Morita, 1982; Foster, 1963; Foster, 1969; Schaeffer, 1993). Interestingly, the observation that neoblast numbers increase after abrogation of PTEN function in planarians, is accompanied by a generalized infiltration of neoblast-like cells in many different organs, which supports this possibility. It is also consistent with previous findings, showing that embryonic stem cells (*PTEN*<sup>-/-</sup>) possess an enhanced capability to produce teratomas, after subcutaneous injections in syngeneic mice with similar histological features (i.e. increased cellularity, and dysplasia mostly composed of small, round undifferentiated cells) (Di Cristofano et al., 1998). Taken together, our findings strongly indicate that the *Smed-PTEN* phenotype provides a novel invertebrate context, in which the autonomous and non-autonomous regulation of tumor suppressors on adult stem cells can be simultaneously analyzed in all the different organs of a whole organism.

### **Controlling abnormal stem cell proliferation by targeting components of the TOR pathway**

The PI3K-Akt-TOR pathway is evolutionarily conserved and it has been shown that loss of PTEN function activates Akt. Because functional abrogation of the *Smed-PTEN* genes led to increases in *Smed-Akt* expression, and because the symptoms of the *Smed-PTEN* phenotype were prevented by rapamycin treatment, components of this pathway are likely to be conserved in *S. mediterranea*. The ability of rapamycin to regulate neoblast numbers, and their differentiation, during homeostasis and

regeneration in the absence of functional *Smed-PTEN* genes, reveals a highly specific mechanism of action for rapamycin, and provides a unique opportunity to explore the mechanisms of action of this macrolide in vivo. Therefore, in planarians, it is possible to target abnormal proliferative cells while retaining an adequate neoblast response to meet physiological demands. This is consistent with recent findings demonstrating that rapamycin treatment compensates for PTEN loss, and is effective in preventing the development of leukemia-initiating cells, while maintaining normal hematopoietic function in mice (Yilmaz et al., 2006). However, the precise mechanism of action by which rapamycin distinguishes between abnormal and physiological stem cell proliferation is not completely understood and will require further analyses. Thus, the identification and characterization of additional, evolutionarily conserved components of the PI3K-Akt-TOR pathway, as well as possible targets of rapamycin, should be possible in planarians.

Even though an important consequence of abrogating *Smed-PTEN* genes was the generalized increase in *Smed-Akt* expression, disruption of *Smed-Akt* function did not prevent the hyperproliferation and visible outgrowths that have been previously reported for this pathway in mammals (Chen et al., 2006). In fact, the only aspect of the *Smed-PTEN* loss-of-function phenotype rescued by abrogation of *Smed-Akt*, is the regression of the area in front of the photoreceptor – a region of the animal devoid of proliferative activity, and which is maintained exclusively by the migration of postmitotic neoblast progeny (Newmark and Sánchez Alvarado, 2000; Reddien et al., 2005b). Interestingly, the highest proportion of *Smed-Akt* expression in *Smed-PTEN-1, -2(RNAi)* animals was observed in the X2 subpopulation of our FACS analyses, which includes migratory differentiating cells (Higuchi et al., 2007; Oviedo and Levin, 2007). Therefore, we propose that the abnormalities observed in the *Smed-PTEN* phenotype, such as head regression, may be associated with an abnormal increase in *Smed-Akt* expression, but others, such as hyperproliferation, lack of regeneration, and abnormal outgrowths are due specifically to the disruption of *Smed-PTEN* function. However, the partial preventative effect of rapamycin treatment in triple RNAi worms suggests that *Akt* is required to mediate rapamycin action in *Smed-PTEN(RNAi)* animals.

## CONCLUSIONS

Taken together, our findings provide insights into the evolution of PTEN, and the regulatory mechanism operating in adult stem cells during homeostasis and regeneration. Moreover, similar to mammalian adult stem cells, planarian neoblasts exists in a tightly regulated environment that allows constant support of differentiated tissues, while keeping the required form and function throughout the life of the organism (Newmark and Sánchez Alvarado, 2002; Reddien and Sánchez Alvarado, 2004; Sánchez Alvarado, 2006). Thus, the *Smed-PTEN* phenotype revealed that components of the neoblast regulatory mechanisms used during proliferation, differentiation and regeneration are conserved between planarians and mammals. As such, it is now possible to use *S. mediterranea* as a model, in which the pathways controlling adult stem cell biology and cellular regulation can be studied during the regeneration of complex structures. Equally important is the fact that abnormal stem cell proliferation can be specifically

induced in *S. mediterranea*, broadening the opportunity to understand the relationship between cancer and stem cells. Future work will exploit the biology of *S. mediterranea* to pursue pharmacological, genetic and physiological approaches to elucidate potential therapeutic targets that could resolve PI3K-Akt-TOR pathway alterations.

## METHODS

### Planarian culture

The clonal asexual strain CIW4 of *Schmidtea mediterranea* was used in all experiments. Animals were kept and maintained as previously described (Cebrià and Newmark, 2005; Sánchez Alvarado et al., 2002).

### *Smed-PTEN* and *Smed-Akt* isolation

*PTEN* homologues *Smed-PTEN-1* and *-2* (accession numbers: AY068282 and AY066355, respectively) were identified in the *Schmidtea mediterranea* database SmedDb (Sánchez Alvarado et al., 2002). 5' RACE was performed to isolate full lengths (Oviedo and Levin, 2007; Reddien et al., 2005b). Genomic sequences were obtained from the ongoing *S. mediterranea* Genome Project (Washington University Genome Sequence Center) to obtain *Smed-Akt* and *Smed-PCNA* sequences.

### Phylogenetic analysis

*PTEN* sequences were aligned with the program T-Coffee (Notredame et al., 2000). Alignments were edited by hand and subject to Bayesian analysis through the freeware program Geneious ([www.geneious.com](http://www.geneious.com)) and the MrBayes plugin (Ronquist and Huelsenbeck, 2003). MrBayes was run with parameters of 1,000,000 generations, 4 chains, a subsample frequency of 500 and burnin of 100,000.

### Gene expression studies

#### Whole-mount ISHs

Samples and probes for ISHs were processed as previously described (Oviedo and Levin, 2007; Reddien et al., 2005b). An optimized in situ protocol was also used for whole-mount analysis and is available upon request. Briefly, planaria are fixed with 4% formaldehyde in PBS, dehydrated and bleached in 6% H<sub>2</sub>O<sub>2</sub> overnight, treated with 3 µg/ml ProteinaseK for 10 minutes, postfixed in 4% formaldehyde for 10 minutes and then subject to previously described hybridization and detection. All images are representative of at least three different experiments and were captured as previously described (Oviedo and Levin, 2007; Oviedo et al., 2003).

#### qRT-PCR

Use of total RNA isolation procedures and internal controls were as previously described (Oviedo and Levin, 2007; Reddien et al., 2005b).

#### ISH on dissociated cells and quantification of positive cells

Planarian dissociation ( $n=10$  per condition) was performed as previously described (Oviedo and Levin, 2007; Reddien et al., 2005b) but without any filtration step. Briefly, dissociated cells were resuspended in equal volumes of calcium magnesium free media (CMF), spotted onto slides and fixed with 4% PFA. ISH was

performed as previously described (Oviedo and Levin, 2007; Reddien et al., 2005b). Nuclear counterstaining was performed with propidium iodide (PI). Cells that were positive for PI and different probes (neoblasts and differentiated tissues) were quantified with a compound scope ( $20\times$  objective) using IPLab software (Olympus). An average of total cell number was obtained from 20 different fields per slide (neoblast markers), or, using a  $20\times$  objective, the total number of positive cells per whole slide was recorded (differentiated tissue markers).

### Planarian dissociation and FACS analyses

Intact animals ( $n\sim 10$  per condition) were dissociated as previously described (Oviedo and Levin, 2007; Reddien et al., 2005b). Either FACSVantage (Becton Dickinson) or MoFlo high-speed cell sorter (Dako) were used to isolate cells. Results were analyzed by using CELL Quest (Becton Dickinson) or Summit (Dako) software (Oviedo and Levin, 2007; Reddien et al., 2005b).

### dsRNA synthesis and microinjections

dsRNA synthesis and microinjections were performed as previously described (Oviedo and Levin, 2007). Microinjection schedules were subjected to extensive rounds of optimization until reproducible results were obtained. Each injection was performed in the prepharyngeal area, consisting of three pulses of 32.2 nL each, at the time intervals depicted in Fig. 2A; Fig. 3A. Triple RNAi worms were injected on three consecutive days with dsRNA-*Smed-Akt*, followed by two days of rest, and then continued with the same schedule described for *Smed-PTEN-1, -2(RNAi)* worms. During the injection schedule, planarians were evaluated daily under the dissecting scope to observe behavioral reaction and external morphology. Signs of phenotypes were recorded when any of the following were first noticed: abnormal photophobic response, tip regression, external overgrowth, or epithelial damage. In most cases, the same number of animals for each condition (control, RNAi of an individual *Smed-PTEN* or simultaneous *Smed-PTEN-RNAi*) were fixed or processed for additional experiments when 50% of the group displayed signs of the phenotype.

### Rapamycin treatment

Rapamycin was obtained from two sources: Calbiochem and Cell Signaling Technology. Concentrated stock was freshly diluted (20 nM) in planarian water before daily prepharyngeal injections (five pulses of 32 nL each per worm). Rapamycin injections were always scheduled for 2–3 hours before respective dsRNA injections.

### Antibody labeling and image collection

Planarians were processed for immunostaining as previously described (Reddien et al., 2005a; Reddien et al., 2005b). Primary antibodies were diluted as follows:  $\alpha$ -phosphorylated histone H3 (Upstate), 1:5000;  $\alpha$ -arrestin (kind gift from K. Agata), 1:5000; anti-planarian myosin heavy chain monoclonal antibody TMUS-13 (kind gift from R. Romero), 1:100;  $\alpha$ -acetylated tubulin monoclonal antibody (Sigma), 1:500; and anti-SMEDWI-1 antibody (kind gift from P. Newmark), 1:1000. Incubation with secondary antibody was performed at room temperature, overnight in goat anti-rabbit Alexa 568, 1:800, or goat anti-mouse Alexa 488, 1:400. At least seven or eight different whole body images were taken per condition to

## TRANSLATIONAL IMPACT

### Clinical issue

Endogenous stem cells are important in the normal physiology of tissues that undergo constant regeneration, such as hematopoietic cells or those lining the gastrointestinal tract. The enhanced proliferative capacity of stem cells is necessary for the regeneration and healing of damaged tissue, but can also lead to cancer. The carcinogenic potential of stem cells is a significant limitation for their potential use in treating disease. Understanding the mechanisms and signaling pathways that allow stem cells to serve in a controlled regenerative capacity is necessary before their safe therapeutic potential can be realized.

The PTEN protein is a key regulator of cell proliferation, differentiation and motility that is frequently mutated in cancer. PTEN exerts its influence on cellular functions by suppressing the PI3-kinase (PI3K) and AKT pathways. In normal cells, PTEN balances PI3-kinase and AKT activities that otherwise would contribute to the genesis of malignant cancer cells.

### Results

Here the planarian is used as a model organism for studying PTEN in stem cells for tissue regeneration. Planarians contain large numbers of adult stem cells (neoblasts) that constantly renew and differentiate into all known planarian cell types.

In the planarian, *Schmidtea mediterranea*, the authors identify two orthologues to the human *PTEN* gene, which they name *Smed-PTEN-1* and *Smed-PTEN-2*. They find the genes expressed in many cell types, including the planarian stem cells. Reduced expression of *Smed-PTEN-1* and *Smed-PTEN-2* encoded proteins using RNAi resulted in abnormal growths, dramatic anatomical changes and the eventual demise of the organism. As in mammals, administration of the drug rapamycin to RNAi-treated worms prevents all of these abnormalities and the death of the animal.

### Implications and future directions

An important finding here is the extent of evolutionary conservation of the PTEN pathway that allows researchers to use planaria as a model organism for stem cell biology. This work demonstrates the fundamental importance of PTEN in cellular proliferation and differentiation processes. Work on the PTEN pathway in this system will advance our understanding of the mechanisms regulating proliferation, migration and motility that are likely operating in the emergence of human cancers. It also expands opportunities to understand the relationship between pathways that similarly regulate cancer growth and stem cell potential.

doi:10.1242/dmm.001123

quantify the H3P signal as previously described (Reddien et al., 2005a; Reddien et al., 2005b). Representative images from each condition were additionally processed using an Olympus Fluoview-300 confocal microscope (Olympus), or as previously described (Oviedo and Levin, 2007).

### ACKNOWLEDGEMENTS

We thank P. Newmark, K. Agata and R. Romero for reagents; J. LaVecchio, B. Girijesh and the Harvard Stem Cell Institute Flow Cytometry Cores for FACS analysis; P. Reddien for sharing protocols, reagents and valuable suggestions; S. Morrison for rapamycin advice; J. Dobeck for histological assistance; R. Kent for assistance with data analysis; J. Jenkin, K. Gallant, D. Qiu and J. Morokuma for lab assistance; and C.-B. Chien and C. Rodesh for advice with imaging. N.J.O. is an NIH fellow supported under Ruth L. Kirschstein National Research Service Award (F32 GM078774). N.J.O. also thanks the Oviedo-Pfister family for encouragement. This work was supported by NSF grant IBN#0347295, NHTSA grant DTNH22-06-G-00001, and NIH grant R21 HD055850 to M.L. and NIH-NIGMS RO-1 GM57260 to A.S.A. B.J.P. is a Damon Runyon Fellow (DRG#1888-05) and A.S.A. is a Howard Hughes Medical Institute Investigator. Part of this research was conducted in a Forsyth Institute facility renovated with support from Research Facilities Improvement Grant Number CO6RR11244 from the National Center for Research Resources, NIH.

## COMPETING INTERESTS STATEMENT

The authors declare no competing financial interests.

## AUTHOR CONTRIBUTIONS

N.J.O. performed and analyzed all of the experiments with the exception of those reported in Fig. 1A-C, which were executed and interpreted by B.J.P. B.J.P. also optimized the whole-mount *in situ* hybridization protocol. A.S.A. and N.J.O. conceived the experiments. A.S.A. and M.L. supervised N.J.O. M.L. contributed reagents and participated in manuscript preparation. A.S.A., N.J.O. and B.J.P. wrote the manuscript.

## SUPPLEMENTARY MATERIAL

Supplementary material for this article is available at <http://dmm.biologists.org/content/1/2-3/131/suppl/DC1>

Received 9 January 2008; Accepted 29 March 2008.

## REFERENCES

- Asano, T., Yao, Y., Zhu, J., Li, D., Abbruzzese, J. L. and Reddy, S. A.** (2004). The PI 3-kinase/Akt signaling pathway is activated due to aberrant Pten expression and targets transcription factors NF-kappaB and c-Myc in pancreatic cancer cells. *Oncogene* **23**, 8571-8580.
- Best, J. and Morita, M.** (1982). Planarians as a model system for *in vitro* teratogenesis studies. *Teratog. Carcinog. Mutagen.* **2**, 277-291.
- Cebrià, F. and Newmark, P. A.** (2005). Planarian homologs of netrin and netrin receptor are required for proper regeneration of the central nervous system and the maintenance of nervous system architecture. *Development* **132**, 3691-3703.
- Cebrià, F., Vispo, M., Bueno, D., Carranza, S., Newmark, P. and Romero, R.** (1996). Myosin heavy chain gene in *Dugesia* (G.) tigrina: a tool for studying muscle regeneration in planarians. *Int. J. Dev. Biol. Suppl.* **1**, 177S-178S.
- Chen, M. L., Xu, P. Z., Peng, X. D., Chen, W. S., Guzman, G., Yang, X., Di Cristofano, A., Pandolfi, P. P. and Hay, N.** (2006). The deficiency of Akt1 is sufficient to suppress tumor development in *Pten* +/- mice. *Genes Dev.* **20**, 1569-1574.
- Clarke, M. F. and Fuller, M.** (2006). Stem cells and cancer: two faces of eve. *Cell* **124**, 1111-1115.
- Di Cristofano, A., Pesce, B., Cordon-Cardo, C. and Pandolfi, P. P.** (1998). Pten is essential for embryonic development and tumour suppression. *Nat. Genet.* **19**, 348-355.
- Foster, J. A.** (1963). Induction of neoplasms in planarians with carcinogens. *Cancer Res.* **23**, 300-303.
- Foster, J. A.** (1969). Malformations and lethal growths in planaria treated with carcinogens. *Natl. Cancer Inst. Monogr.* **31**, 683-691.
- Gao, X., Neufeld, T. P. and Pan, D.** (2000). Drosophila PTEN regulates cell growth and proliferation through PI3K-dependent and -independent pathways. *Dev. Biol.* **221**, 404-418.
- Gil, E. B., Malone Link, E., Liu, L. X., Johnson, C. D. and Lees, J. A.** (1999). Regulation of the insulin-like developmental pathway of *Caenorhabditis elegans* by a homolog of the PTEN tumor suppressor gene. *Proc. Natl. Acad. Sci. USA* **96**, 2925-2930.
- Goberdhan, D. C., Paricio, N., Goodman, E. C., Mlodzik, M. and Wilson, C.** (1999). Drosophila tumor suppressor PTEN controls cell size and number by antagonizing the Chico/PI3-kinase signaling pathway. *Genes Dev.* **13**, 3244-3258.
- Gu, J., Tamura, M. and Yamada, K. M.** (1998). Tumor Suppressor PTEN Inhibits Integrin- and Growth Factor-mediated Mitogen-activated Protein (MAP) Kinase Signaling Pathways. *J. Cell Biol.* **143**, 1375-1383.
- Guertin, D. A. and Sabatini, D. M.** (2007). Defining the Role of mTOR in Cancer. *Cancer Cell* **12**, 9-22.
- Guo, T., Peters, A. H. and Newmark, P. A.** (2006). A bruno-like Gene Is Required for Stem Cell Maintenance in Planarians. *Dev. Cell* **11**, 159-169.
- Hafen, E.** (2004). Cancer, type 2 diabetes, and ageing: news from flies and worms. *Swiss Med. Wkly* **134**, 711-719.
- Hayashi, T., Asami, M., Higuchi, S., Shibata, N. and Agata, K.** (2006). Isolation of planarian X-ray-sensitive stem cells by fluorescence-activated cell sorting. *Dev. Growth Differ.* **48**, 371-380.
- Higuchi, S., Hayashi, T., Hori, I., Shibata, N., Sakamoto, H. and Agata, K.** (2007). Characterization and categorization of fluorescence activated cell sorted planarian stem cells by ultrastructural analysis. *Dev. Growth Differ.* **49**, 571-581.
- Hori, I.** (1979a). Regeneration of the epidermis and basement membrane of the planarian *Dugesia japonica* after total-body X irradiation. *Radiat. Res.* **77**, 521-533.
- Hori, I.** (1979b). Structure and regeneration of the planarian basal lamina: an ultrastructural study. *Tissue Cell* **11**, 611-621.
- Hori, I.** (1980). Localization of newly synthesized precursors of basal lamina in the regenerating planarian as revealed by autoradiography. *Tissue Cell* **12**, 513-521.
- Huang, H., Potter, C. J., Tao, W., Li, D. M., Brogiolo, W., Hafen, E., Sun, H. and Xu, T.** (1999). PTEN affects cell size, cell proliferation and apoptosis during Drosophila eye development. *Development* **126**, 5365-5372.
- Janzen, V. and Scadden, D. T.** (2006). Stem cells: good, bad and reformable. *Nature* **441**, 418-419.
- Kirkegaard, T., Witton, C. J., McGlynn, L. M., Tovey, S. M., Dunne, B., Lyon, A. and Bartlett, J. M.** (2005). AKT activation predicts outcome in breast cancer patients treated with tamoxifen. *J Pathol* **207**, 139-146.
- Lee, J. O., Yang, H., Georgescu, M. M., Di Cristofano, A., Maehama, T., Shi, Y., Dixon, J. E., Pandolfi, P. and Pavletich, N. P.** (1999). Crystal structure of the PTEN tumor suppressor: implications for its phosphoinositide phosphatase activity and membrane association. *Cell* **99**, 323-334.
- Li, J., Yen, C., Liaw, D., Podsypanina, K., Bose, S., Wang, S. I., Puc, J., Miliaresis, C., Rodgers, L., McCombie, R. et al.** (1997). PTEN, a putative protein tyrosine phosphatase gene mutated in human brain, breast, and prostate cancer. *Science* **275**, 1943-1947.
- Liaw, D., Marsh, D. J., Li, J., Dahia, P. L., Wang, S. I., Zheng, Z., Bose, S., Call, K. M., Tsou, H. C., Peacocke, M. et al.** (1997). Germline mutations of the PTEN gene in Cowden disease, an inherited breast and thyroid cancer syndrome. *Nat. Genet.* **16**, 64-67.
- Marsh, D. J., Dahia, P. L., Zheng, Z., Liaw, D., Parsons, R., Gorlin, R. J. and Eng, C.** (1997). Germline mutations in PTEN are present in Bannayan-Zonana syndrome. *Nat. Genet.* **16**, 333-334.
- Marsh, D. J., Kum, J. B., Lunetta, K. L., Bennett, M. J., Gorlin, R. J., Ahmed, S. F., Bodurtha, J., Crowe, C., Curtis, M. A., Dasouki, M. et al.** (1999). PTEN mutation spectrum and genotype-phenotype correlations in Bannayan-Riley-Ruvalcaba syndrome suggest a single entity with Cowden syndrome. *Hum. Mol. Genet.* **8**, 1461-1472.
- Marx, J.** (2007). Molecular biology. Cancer's perpetual source? *Science* **317**, 1029-1031.
- Mihaylova, V. T., Borland, C. Z., Manjarrez, L., Stern, M. J. and Sun, H.** (1999). The PTEN tumor suppressor homolog in *Caenorhabditis elegans* regulates longevity and dauer formation in an insulin receptor-like signaling pathway. *Proc. Natl. Acad. Sci. USA* **96**, 7427-7432.
- Nakahara, Y., Nagai, H., Kinoshita, T., Uchida, T., Hatano, S., Murate, T. and Saito, H.** (1998). Mutational analysis of the PTEN/MMAC1 gene in non-Hodgkin's lymphoma. *Lymphoma* **12**, 1277-1280.
- Nelen, M. R., van Staveren, W. C., Peeters, E. A., Hassel, M. B., Gorlin, R. J., Hamm, H., Lindboe, C. F., Fryns, J. P., Sijmons, R. H., Woods, D. G. et al.** (1997). Germline mutations in the PTEN/MMAC1 gene in patients with Cowden disease. *Hum. Mol. Genet.* **6**, 1383-1387.
- Nelson, C. M. and Bissell, M. J.** (2006). Of extracellular matrix, scaffolds, and signaling: tissue architecture regulates development, homeostasis, and cancer. *Annu. Rev. Cell Dev. Biol.* **22**, 287-309.
- Newmark, P. and Sánchez Alvarado, A.** (2000). Bromodeoxyuridine specifically labels the regenerative stem cells of planarians. *Dev. Biol.* **220**, 142-153.
- Newmark, P. A. and Sánchez Alvarado, A.** (2002). Not your father's planarian: a classic model enters the era of functional genomics. *Nat. Rev. Genet.* **3**, 210-219.
- Notredame, C., Higgins, D. G. and Heringa, J.** (2000). T-Coffee: A novel method for fast and accurate multiple sequence alignment. *J. Mol. Biol.* **302**, 205-217.
- Ogg, S. and Ruvkun, G.** (1998). The *C. elegans* PTEN homolog, DAF-18, acts in the insulin receptor-like metabolic signaling pathway. *Mol. Cell* **2**, 887-893.
- Oldham, S., Stocker, H., Laffargue, M., Wittwer, F., Wymann, M. and Hafen, E.** (2002). The Drosophila insulin/IGF receptor controls growth and size by modulating PtdInsP(3) levels. *Development* **129**, 4103-4109.
- Oviedo, N. J. and Levin, M.** (2007). smedinx-11 is a planarian stem cell gap junction gene required for regeneration and homeostasis. *Development* **134**, 3121-3131.
- Oviedo, N. J., Newmark, P. A. and Sánchez Alvarado, A.** (2003). Allometric scaling and proportion regulation in the freshwater planarian *Schmidtea mediterranea*. *Dev. Dyn.* **266**, 326-333.
- Polyak, K. and Hahn, W. C.** (2006). Roots and stems: stem cells in cancer. *Nat. Med.* **12**, 296-300.
- Reddien, P. W., Bermange, A. L., Murfitt, K. J., Jennings, J. R. and Sánchez Alvarado, A.** (2005a). Identification of genes needed for regeneration, stem cell function, and tissue homeostasis by systematic gene perturbation in planaria. *Dev. Cell* **8**, 635-649.
- Reddien, P. W., Oviedo, N. J., Jennings, J. R., Jenkins, J. C. and Sánchez Alvarado, A.** (2005b). SMEDWI-2 is a PIWI-like protein that regulates planarian stem cells. *Science* **310**, 1327-1330.
- Reddien, P. W. and Sánchez Alvarado, A.** (2004). Fundamentals of planarian regeneration. *Annu. Rev. Cell Dev. Biol.* **20**, 725-757.
- Reya, T. and Clevers, H.** (2005). Wnt signalling in stem cells and cancer. *Nature* **434**, 843-850.
- Robb, S. M. and Sánchez Alvarado, A.** (2002). Identification of immunological reagents for use in the study of freshwater planarians by means of whole-mount immunofluorescence and confocal microscopy. *Genesis* **32**, 293-298.

- Ronquist, F. and Huelsenbeck, J. P.** (2003). MrBayes 3, Bayesian phylogenetic inference under mixed models. *Bioinformatics* **19**, 1572-1574.
- Rossi, D. J. and Weissman, I. L.** (2006). Pten, tumorigenesis, and stem cell self-renewal. *Cell* **125**, 229-231.
- Sabatini, D. M.** (2006). mTOR and cancer: insights into a complex relationship. *Nat. Rev. Cancer* **6**, 729-734.
- Sakai, F., Agata, K., Orii, H. and Watanabe, K.** (2000). Organization and regeneration ability of spontaneous supernumerary eyes in planarians -eye regeneration field and pathway selection by optic nerves-. *Zool. Sci.* **17**, 375-381.
- Sánchez Alvarado, A.** (2006). Planarian regeneration: its end is its beginning. *Cell* **124**, 241-245.
- Sánchez Alvarado, A. and Newmark, P. A.** (1999). Double-stranded RNA specifically disrupts gene expression during planarian regeneration. *Proc. Natl. Acad. Sci. USA* **96**, 5049-5054.
- Sánchez Alvarado, A., Newmark, P. A., Robb, S. M. and Juste, R.** (2002). The Schmidtea mediterranea database as a molecular resource for studying platyhelminthes, stem cells and regeneration. *Development* **129**, 5659-5665.
- Sansal, I. and Sellers, W. R.** (2004). The biology and clinical relevance of the PTEN tumor suppressor pathway. *J. Clin. Oncol.* **22**, 2954-2963.
- Schaeffer, D. J.** (1993). Planarians as a model system for in vivo tumorigenesis studies. *Ecotoxicol. Environ. Saf.* **25**, 1-18.
- Stiles, B., Groszer, M., Wang, S., Jiao, J. and Wu, H.** (2004). PTENless means more. *Dev. Biol.* **273**, 175-184.
- Sulis, M. L. and Parsons, R.** (2003). PTEN: from pathology to biology. *Trends Cell Biol.* **13**, 478-483.
- Yilmaz, O. H., Valdez, R., Theisen, B. K., Guo, W., Ferguson, D. O., Wu, H. and Morrison, S. J.** (2006). Pten dependence distinguishes haematopoietic stem cells from leukaemia-initiating cells. *Nature* **441**, 475-482.
- Zhang, J., Grindley, J. C., Yin, T., Jayasinghe, S., He, X. C., Ross, J. T., Haug, J. S., Rupp, D., Porter-Westpfahl, K. S., Wiedemann, L. M. et al.** (2006). PTEN maintains haematopoietic stem cells and acts in lineage choice and leukaemia prevention. *Nature* **441**, 518-522.

Figure S1, Oviedo et al.

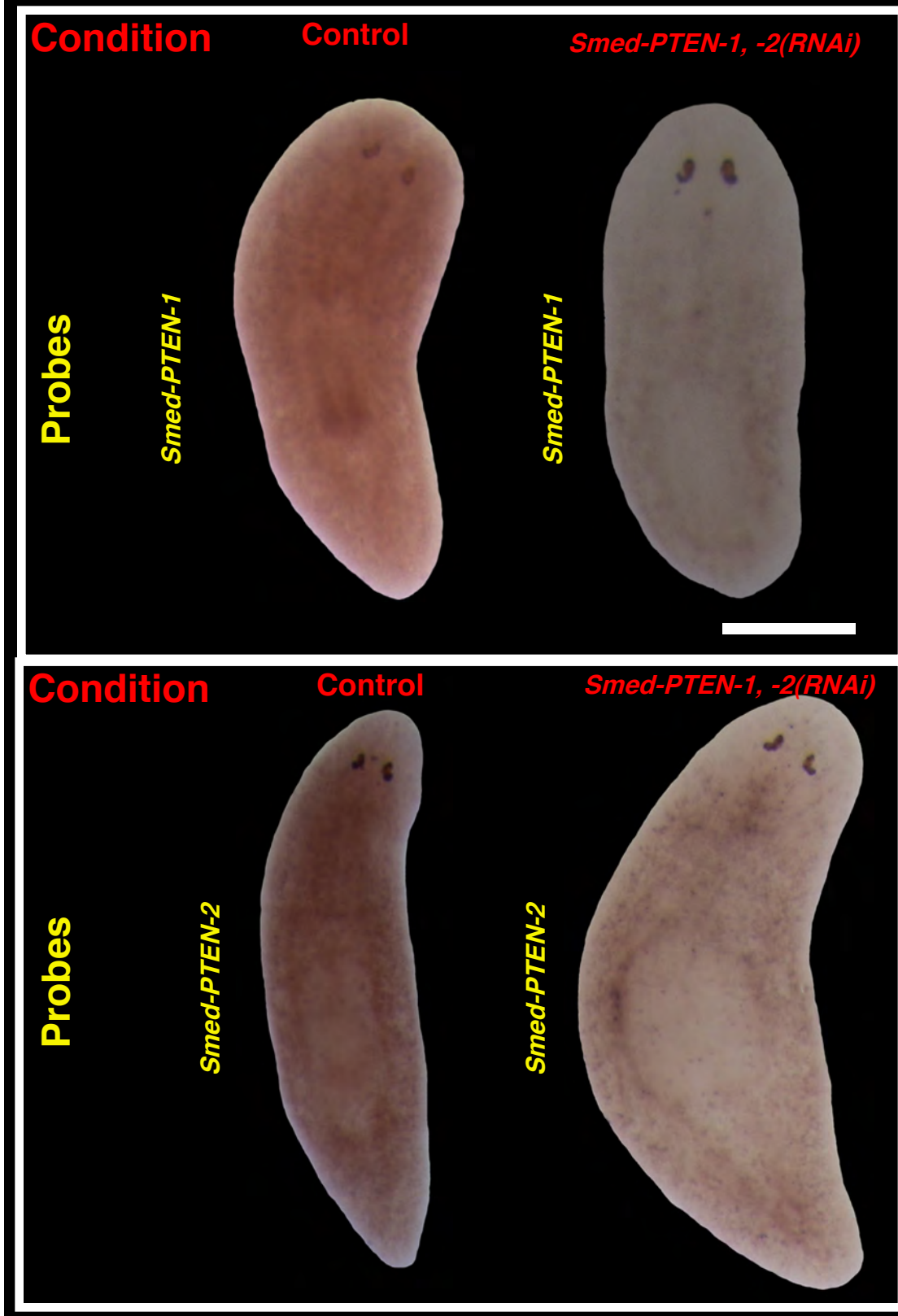
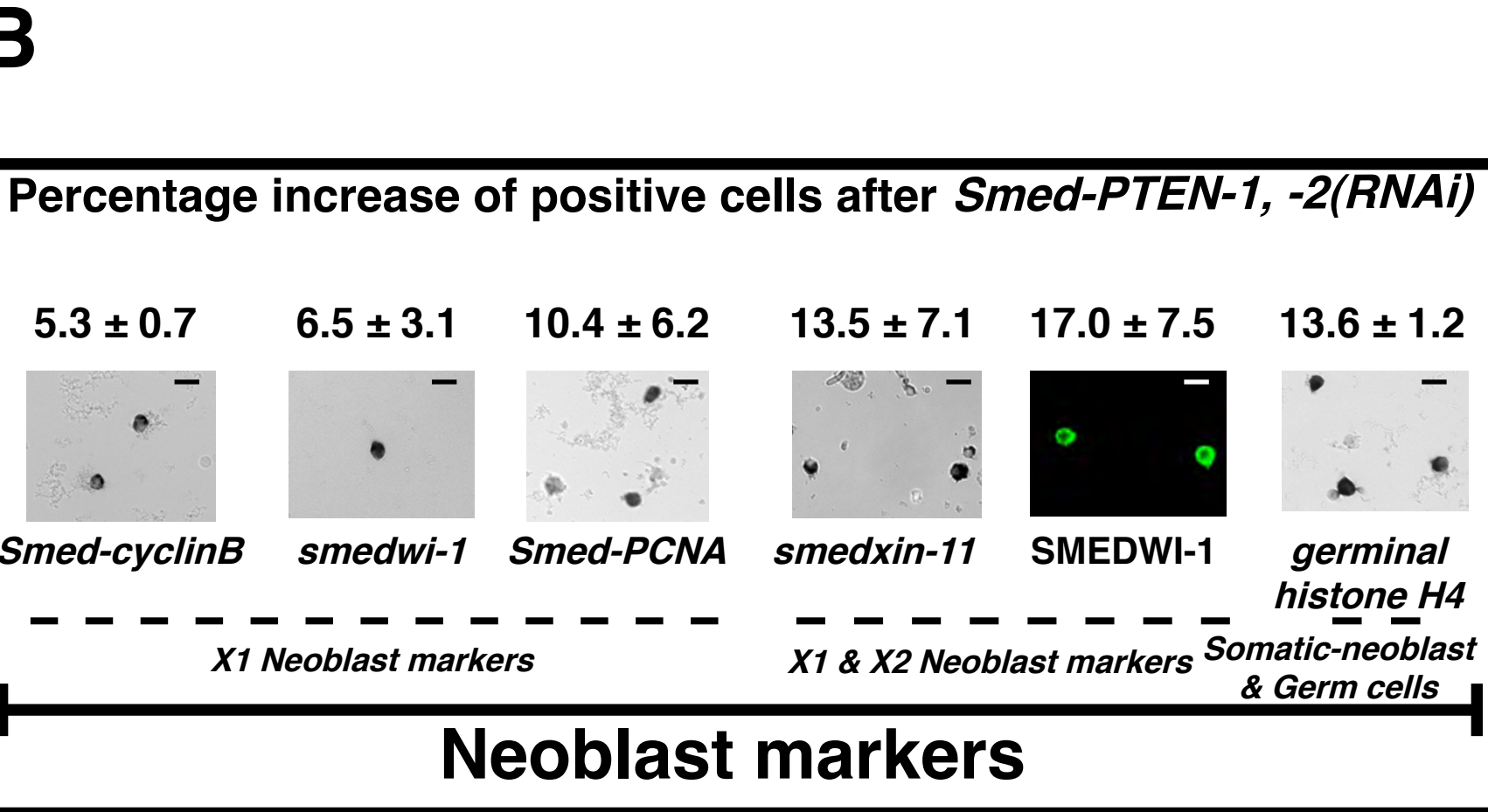
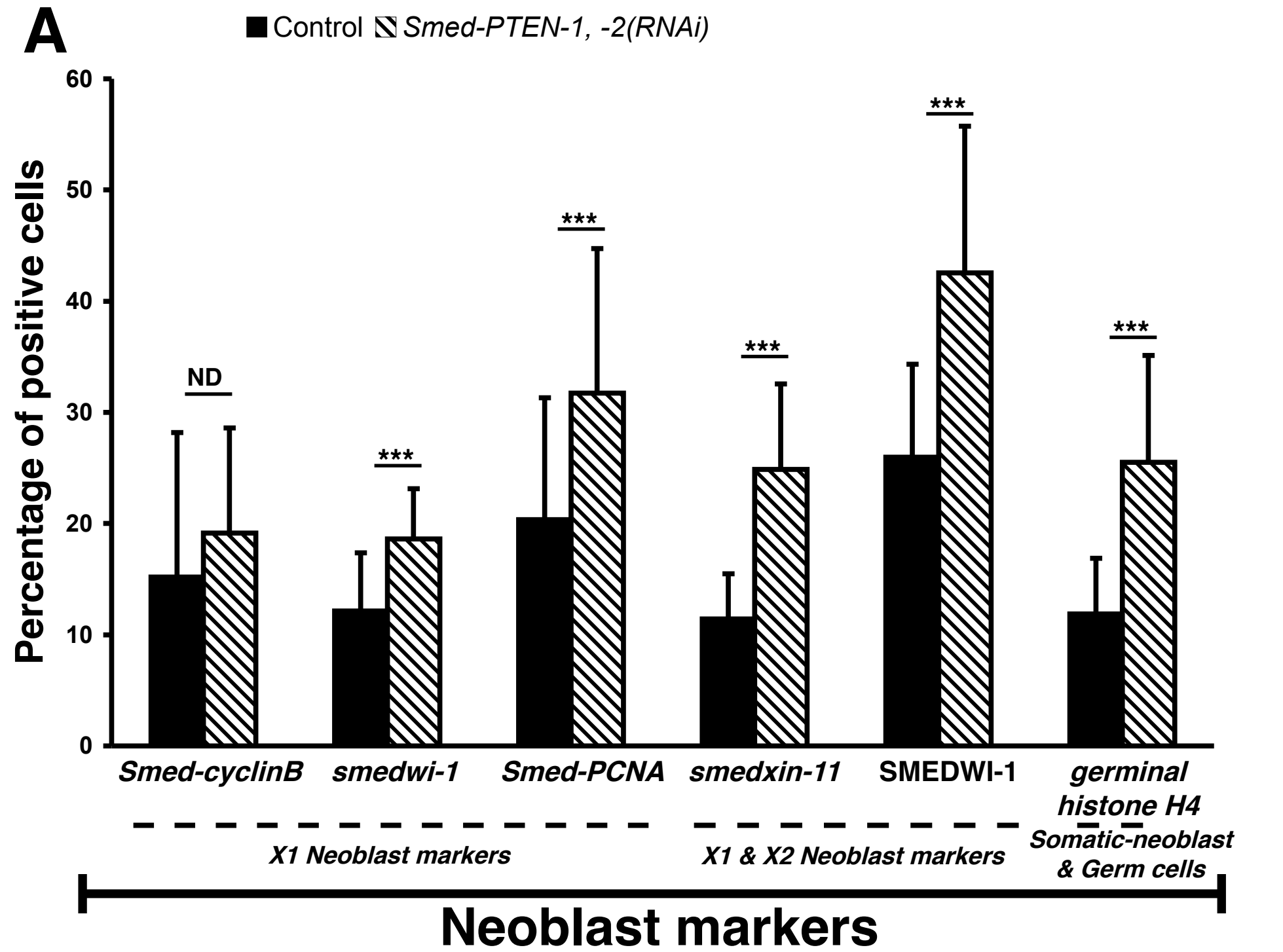
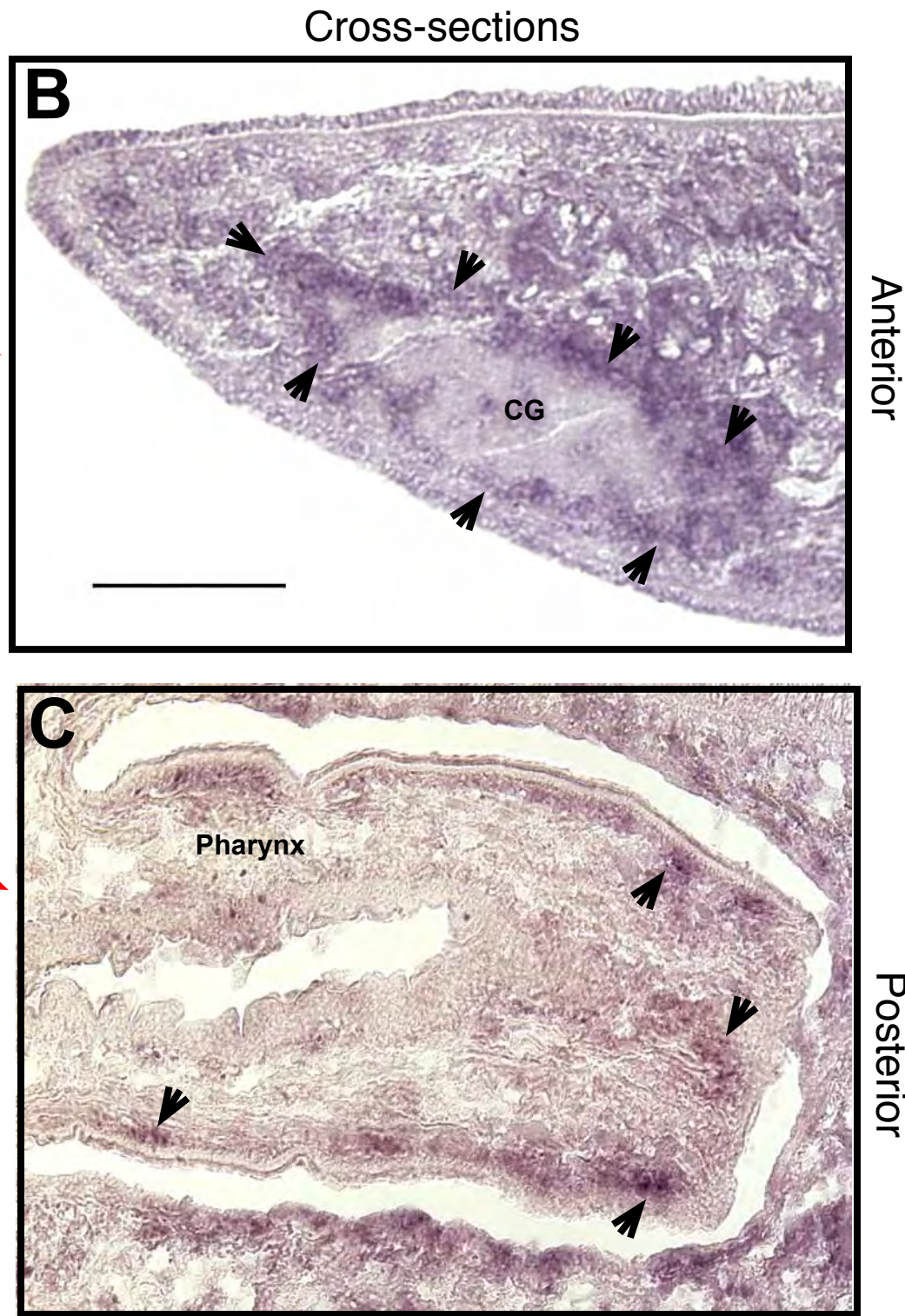
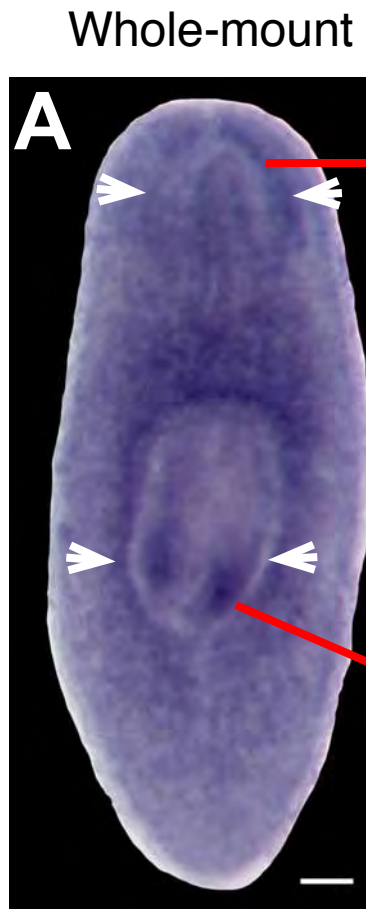


Figure S2, Oviedo et al.



*Smed-Akt* spatial expression

10 days after 1st injection



<i>Smed-PTEN-1, -2(RNAi)</i>	-	-	-	+	+	+
Rapamycin	-	-	-	-	-	+
<i>Smed-Akt(RNAi)</i>	-	+	-	-	+	+

**Table S1.** *Smed-PTEN* phenotype manifestation in intact and regenerating worms

Condition	Phenotype manifestation days after first injection*	Phenotype manifestation days of regeneration*
Intact	10.9 ± 2.2	N/A
Regeneration	10 ± 0.8	2 ± 0.8

\*Represent mean of > four different experiments ± s.d. in which signs of phenotype were macroscopically evident. Total animals evaluated for intact ( $n>100$ ) and regenerating fragments ( $n=47$ ). Phenotype manifestation (days) for intact and regenerating fragments  $p= 0.25$ , Student's *t*-test. Note: In both conditions intact and regeneration 100% of all worms manifested the phenotype and died.

**Table S2.** Expression levels of differentiated tissue markers after *Smed-PTEN-1(RNAi)*; *Smed-PTEN-2(RNAi)*

<b>Gene name</b>	<b>Control</b>	<b><i>Smed-PTEN-1(RNAi);</i> <i>Smed-PTEN-2(RNAi)</i></b>
<i>Smed-SYT</i>	$0.4 \pm 1.9\text{e-}4$	$0.01 \pm 6\text{e-}6$
<i>Smed-CA</i>	$0.18 \pm 2.5\text{e-}3$	0.03
<i>H.1.3b</i>	$1.22 \pm 1.7\text{e-}3$	$1\text{e-}4 \pm 2.2\text{e-}5$
<i>Smed-PTEN-1</i>	$0.07 \pm 7\text{e-}4$	4e-4
<i>Smed-PTEN-2</i>	$0.15 \pm 7\text{e-}5$	$5\text{e-}4 \pm 1.3\text{e-}5$

Results represent mean  $\pm$  SD of two experiments. Data are relative to expression detected for the ubiquitously expressed control *H.55.12e*. See methods for details.